Budker INP Free Electron Laser Facility

Current Status and Future Prospects

O.A. Shevchenko

BINP, Novosibirsk, Russia

RuPAC 2012, 24 - 28 September, Saint-Petersburg

NovoFEL Team

N.A.Vinokurov, V.S.Arbuzov, K.N.Chernov, E.N.Dementyev, B.A.Dovzhenko, Ya.V.Getmanov, E.I.Gorniker, B.A.Knyazev, E.I.Kolobanov, A.A.Kondakov, V.R.Kozak, E.V.Kozyrev, V.V.Kubarev, G.N.Kulipanov, E.A.Kuper, I.V.Kuptsov, G.Ya.Kurkin, L.E.Medvedev, L.A.Mironenko, V.K. Ovchar, B.Z.Persov, A.M.Pilan, V.M.Popik, V.V.Repkov, T.V.Salikova, M.A.Scheglov, I.K.Sedlyarov, G.V.Serdobintsev, S.S.Serednyakov, A.N.Skrinsky, S.V.Tararyshkin, V.G.Tcheskidov, M.G.Vlasenko, P.D.Vobly, V.N.Volkov, O.A.Shevchenko

Outline

- FEL principle of operation
- Accelerator design overview
- The first stage of the FEL facility – design and operation experience
- The second and the third stages – design and commissioning status
- Nearest plans

FEL principle of operation

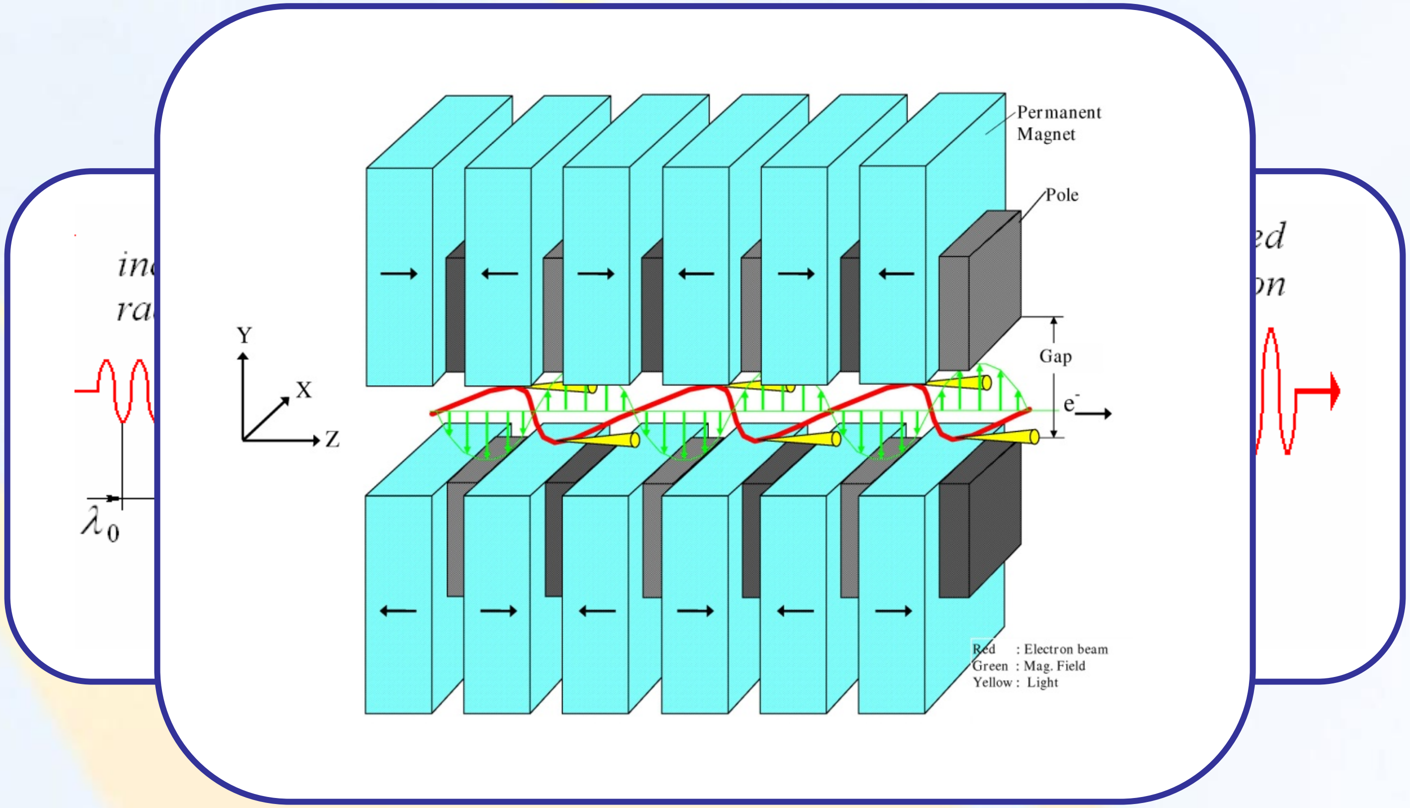

FEL principle of operation

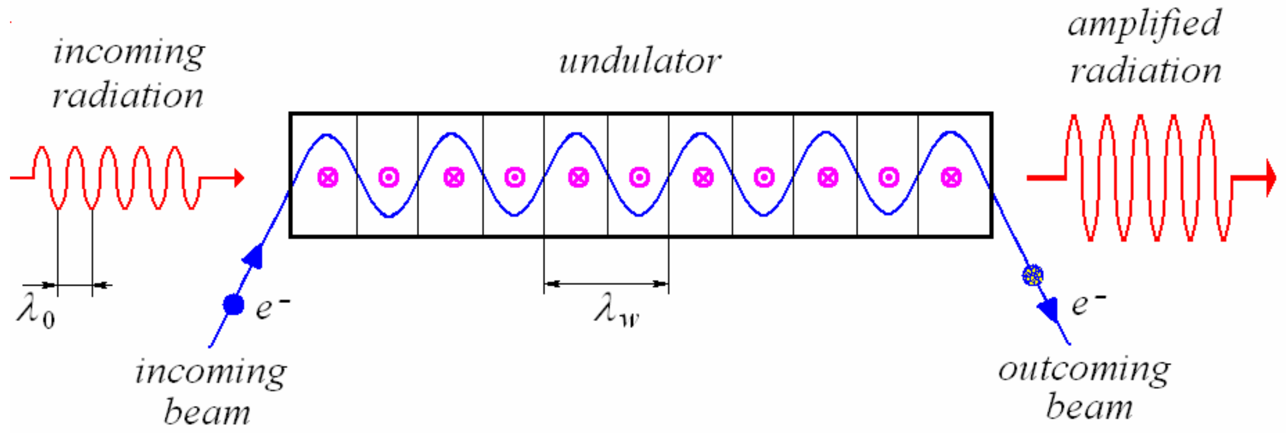

FEL principle of operation

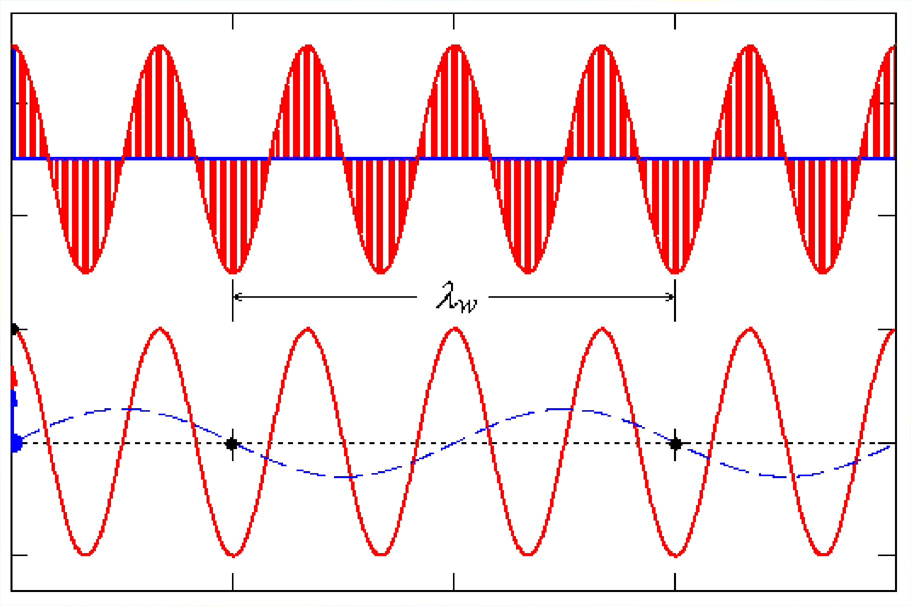

$$\boxed{\lambda_0 \approx \frac{\lambda_w}{2\gamma^2}\left(1+\frac{K^2}{2}\right)}$$

synchronisme condition

which is necessary for the

energy transfer

$$\boxed{\left\langle \frac{d\gamma}{dz} \right\rangle = \frac{e}{mc^3}\langle \mathcal{E}_x V_x \rangle}$$

FEL principle of operation

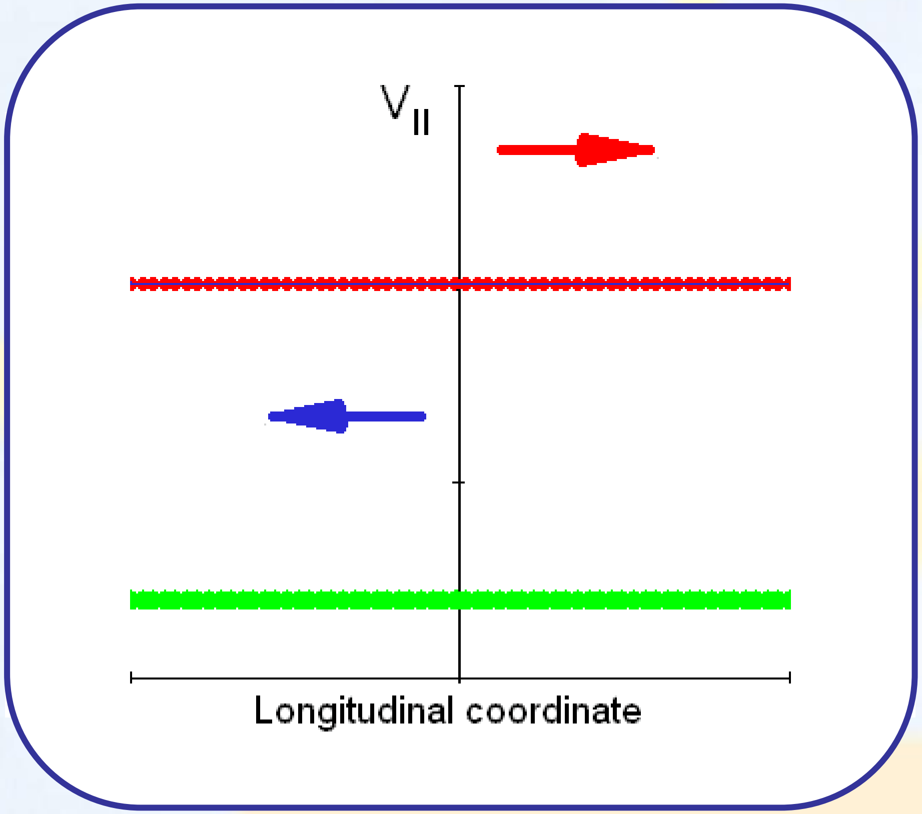

$$\lambda_0 \approx \frac{\lambda_w}{2\gamma^2}\left(1+\frac{K^2}{2}\right)$$

synchronisme condition

which is necessary for the

energy transfer

$$\left\langle \frac{d\gamma}{dz} \right\rangle = \frac{e}{mc^3}\left\langle \mathcal{E}_x V_x \right\rangle$$

FEL principle of operation

FEL oscillator

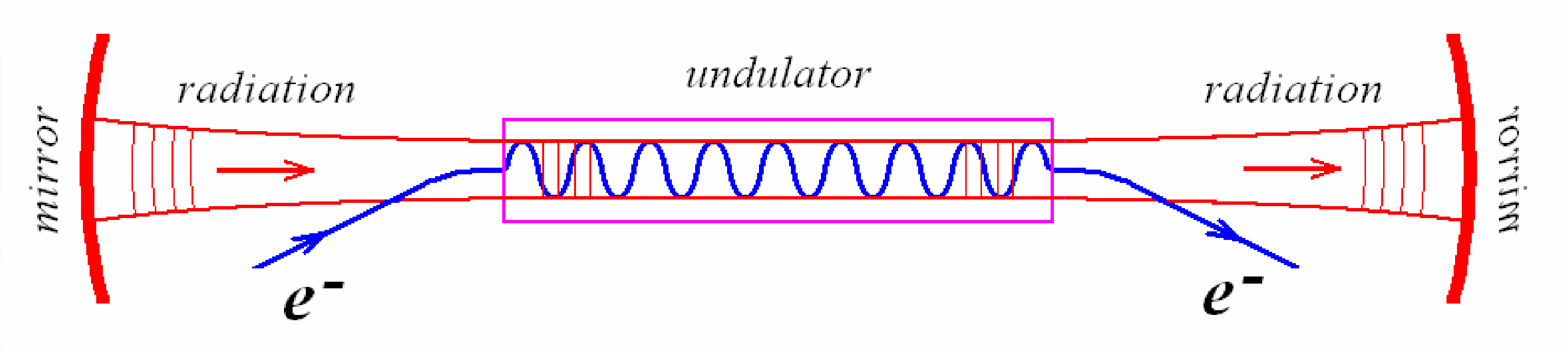

Equivalent scheme

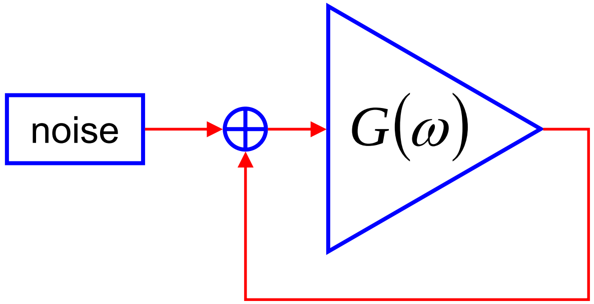

Narrow bandwidth amplifier with feedback

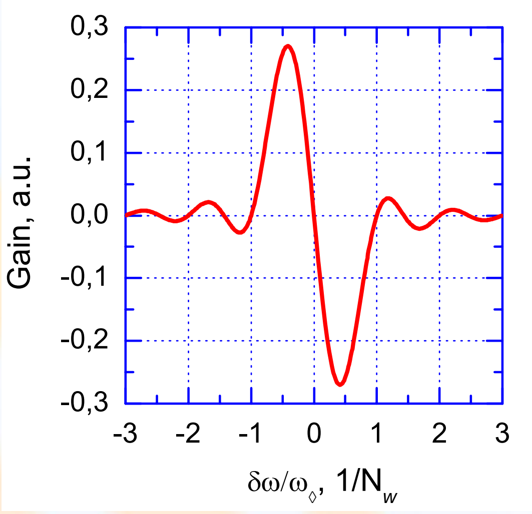

Energy Recovery Linac

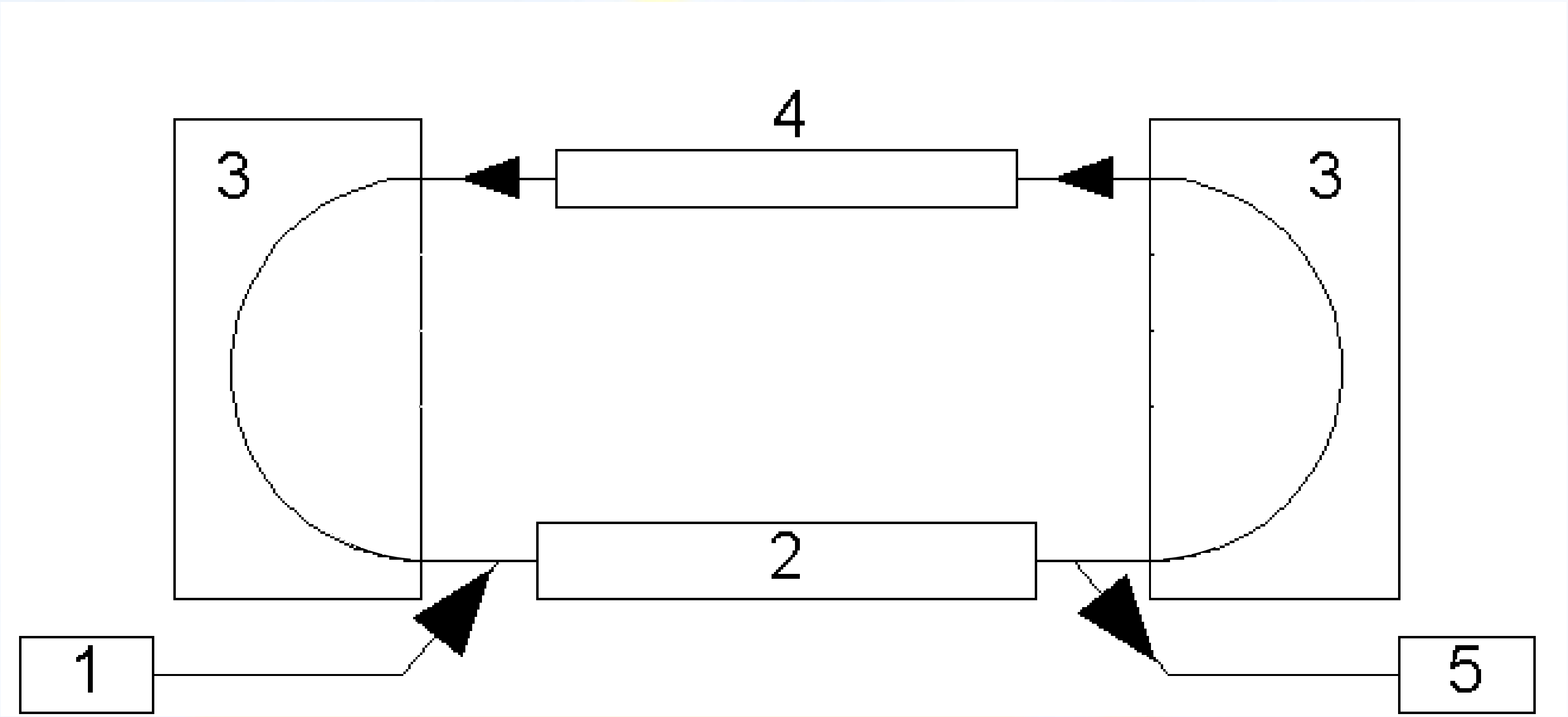

1 – injector, 2 – linac, 3 – bending magnets,
4 – undulator, 5 – dump

Energy Recovery Linac

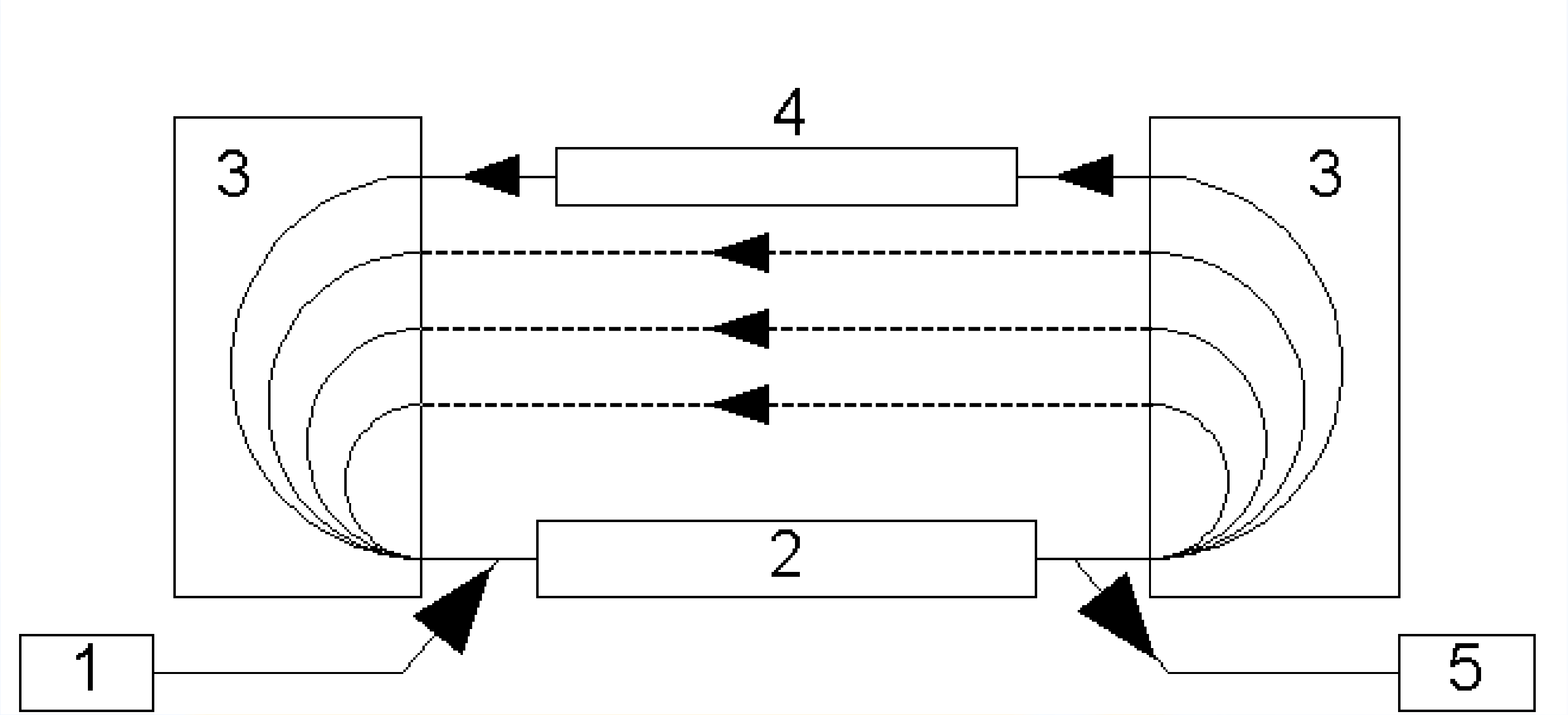

1 – injector, 2 – linac, 3 – bending magnets,
4 – undulator, 5 – dump

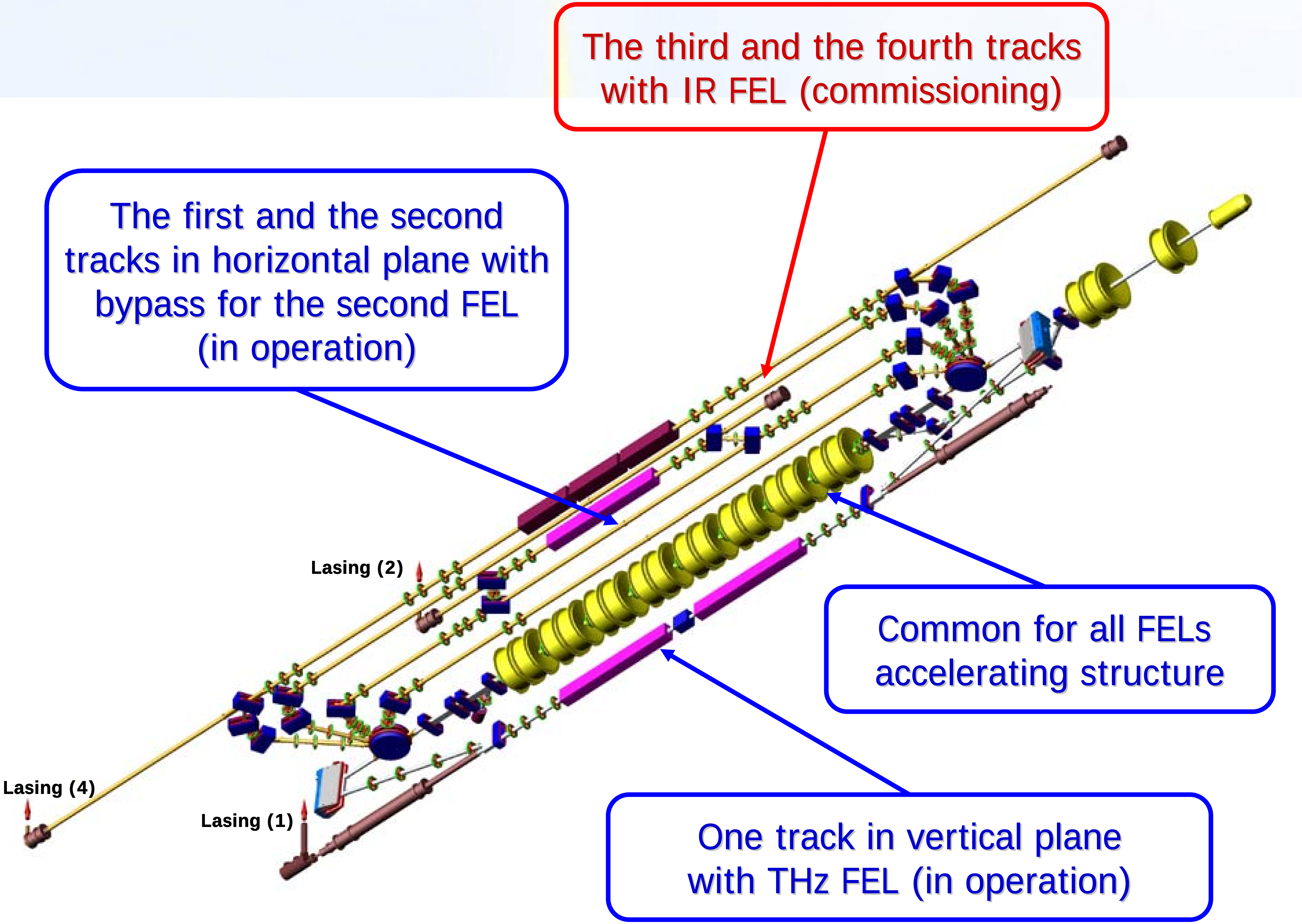
The third and the fourth tracks with IR FEL (commissioning)
The first and the second tracks in horizontal plane with bypass for the second FEL (in operation)
Lasing (2)
Lasing (4)
Lasing (1)
Common for all FELs accelerating structure
One track in vertical plane with THz FEL (in operation)

Siberian Center of Photochemical Research

Siberian Center of Photochemical Research

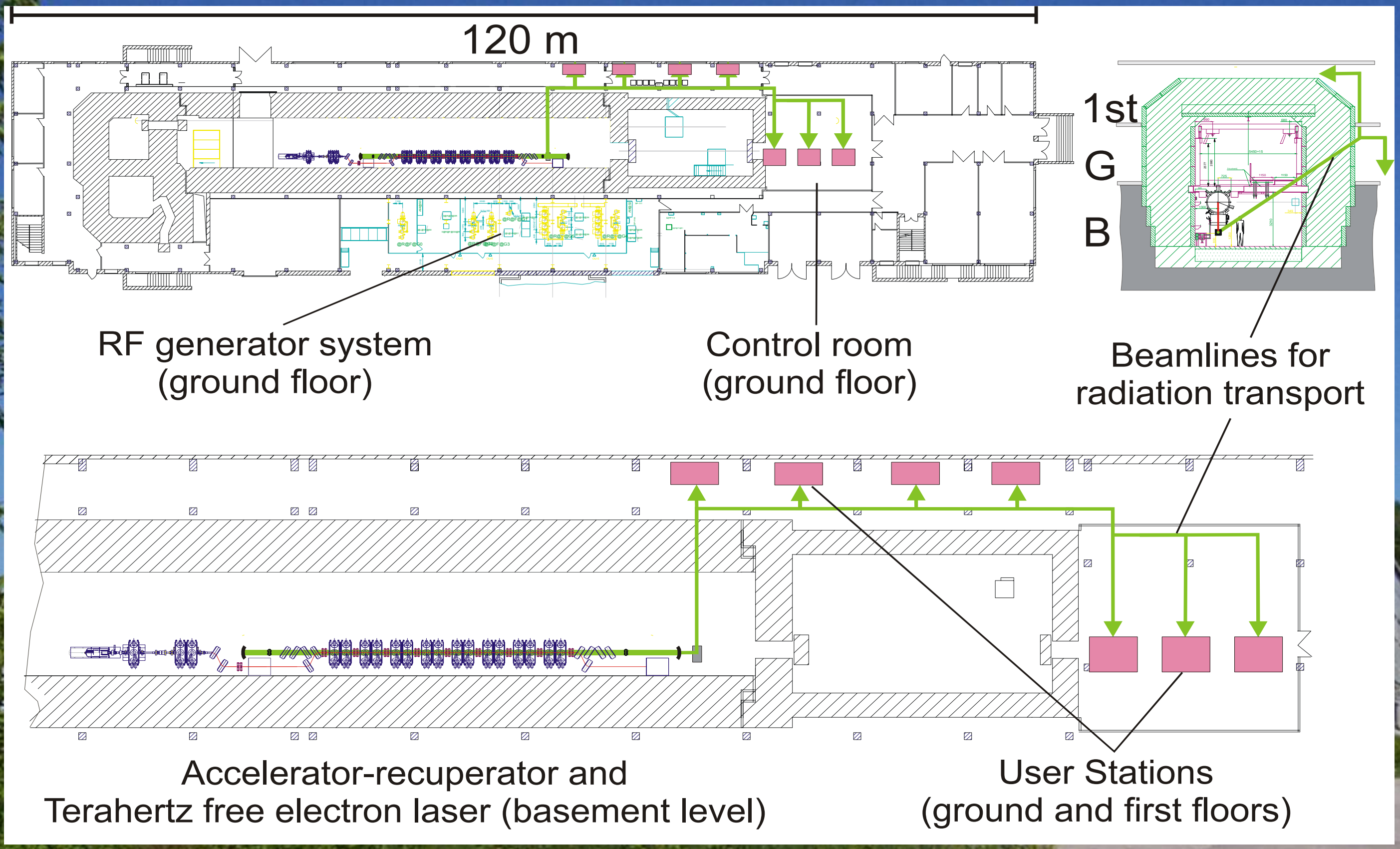

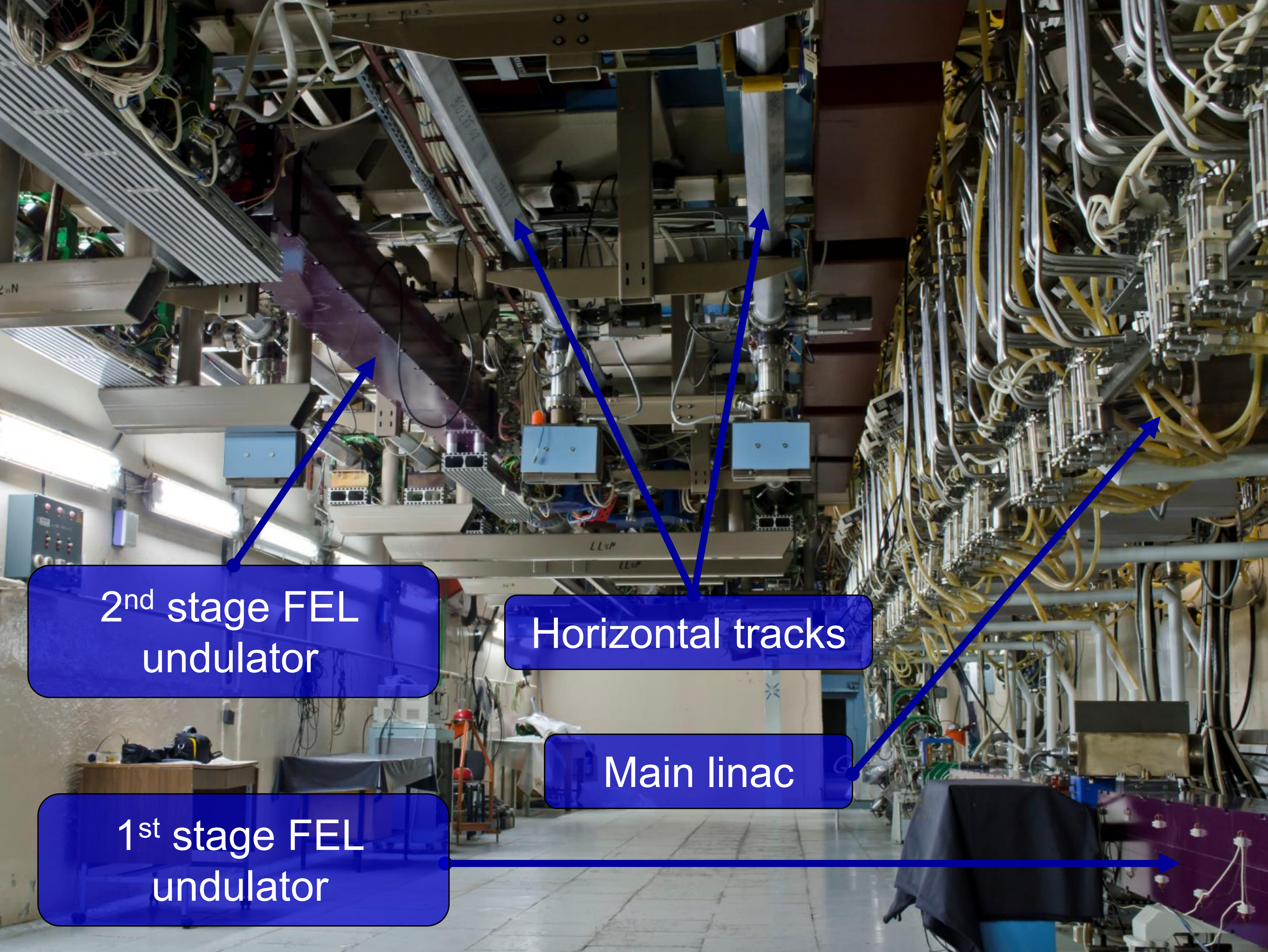
2nd stage FEL undulator
Horizontal tracks
Main linac
1st stage FEL undulator

Injector, main linac and first stage beamlines

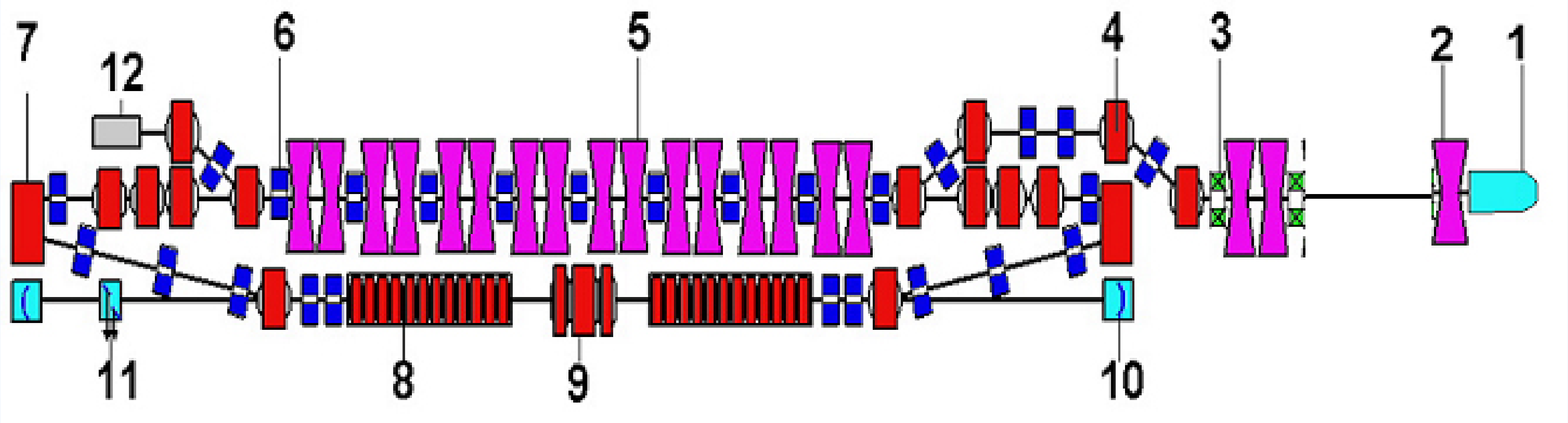

1 – electron gun, 2 – bunching RF cavity, 3 – focusing solenoids, 4 – merger, 5 – main linac, 6 – quadrupoles, 7 – magnetic mirror, 8 - undulator, 9 - buncher, 10 – optical cavity mirror, 11 – calorimeter , 12 - dump.

Electron beam from the gun passes through the buncher (a bunching RF cavity), drift section, 2 MeV accelerating cavities and the main accelerating structure and the undulator, where a fraction of its energy is converted to radiation.

After that, the beam returns to the main accelerating structure in a decelerating RF phase, decreases its energy to its injection value (2 MeV) and is absorbed in the beam dump.

Electrostatic gun

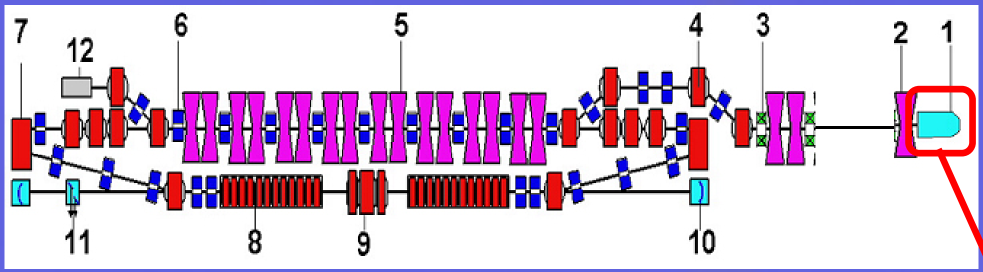

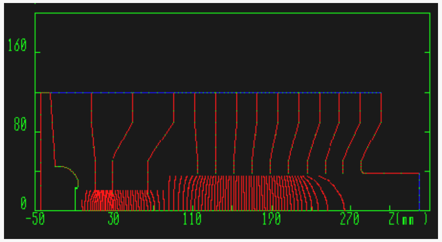

Power supply:

U_{max} = 300 kV

I_{max} = 50 mA

90 MHz RF gun test setup

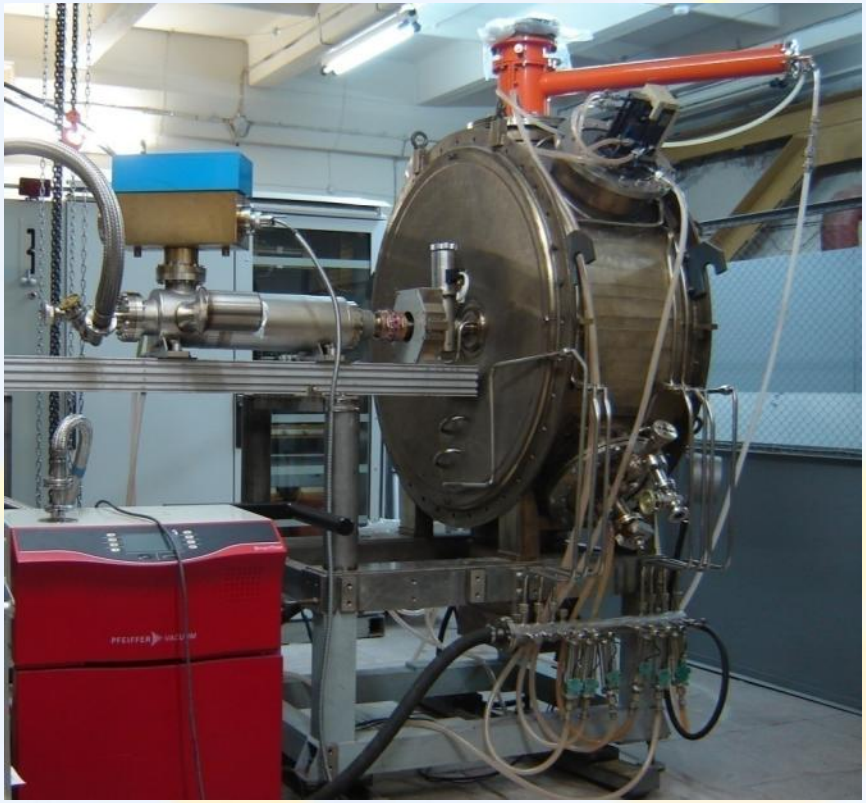

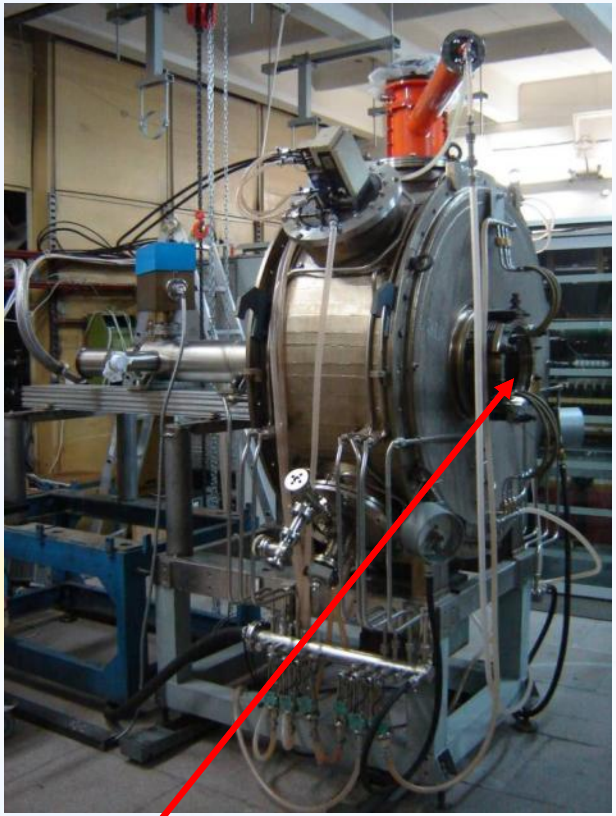

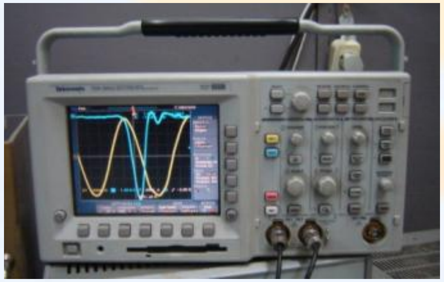

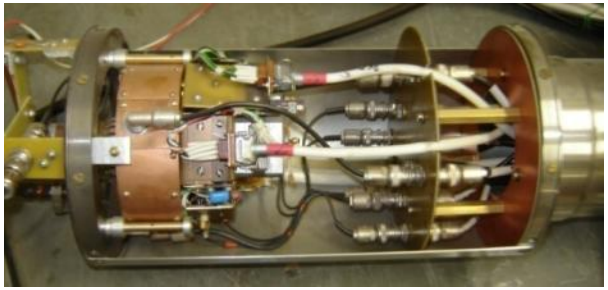

Injector

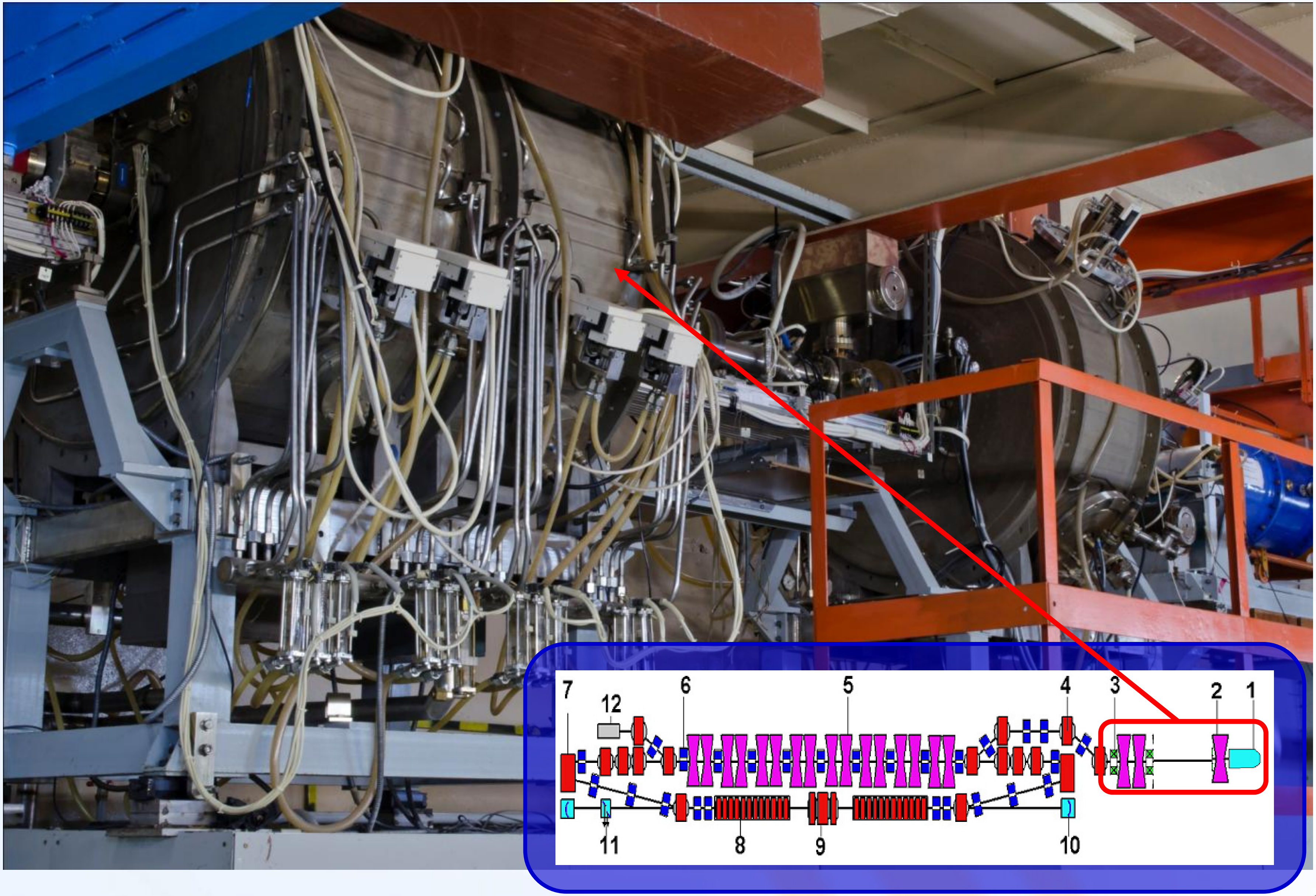

Injector

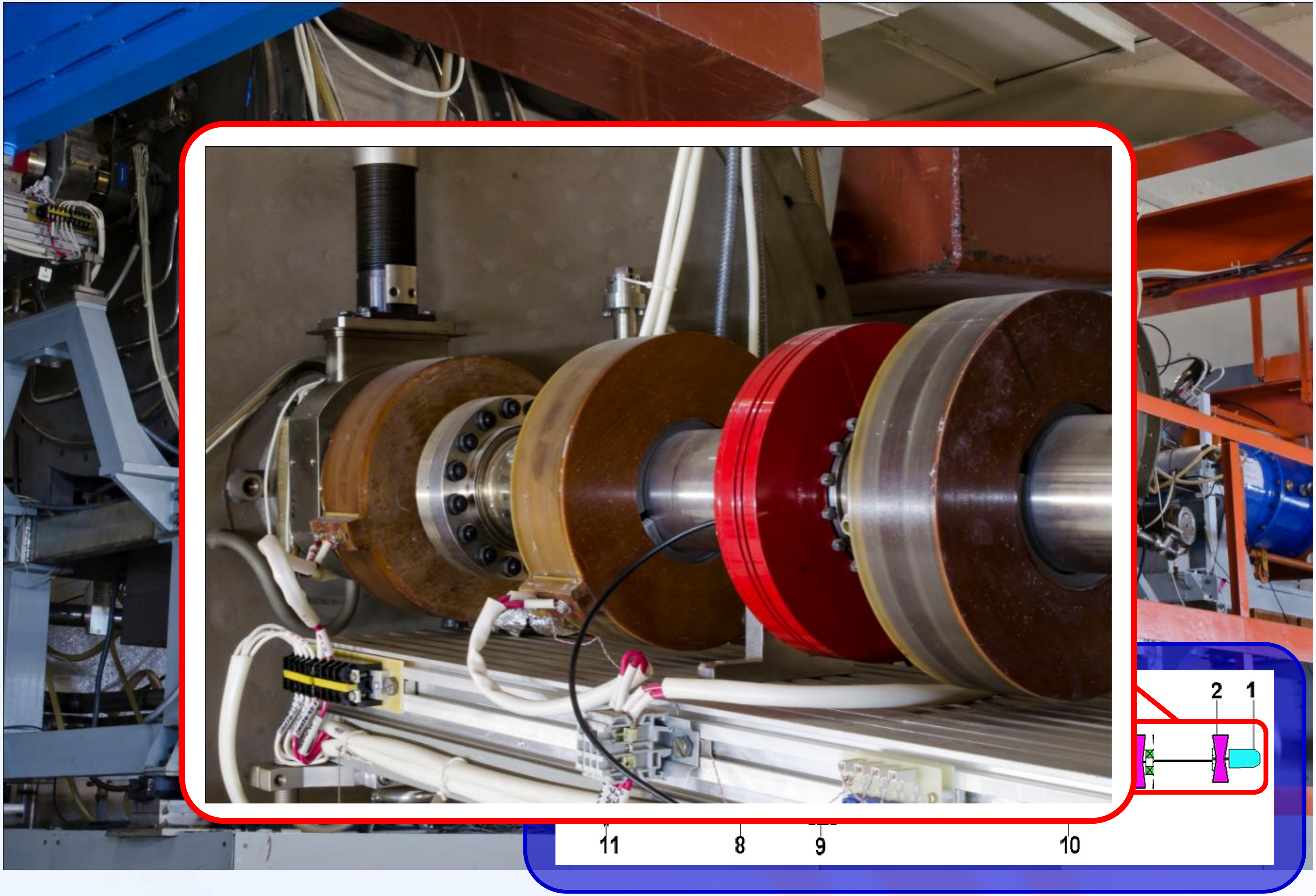

Main linac

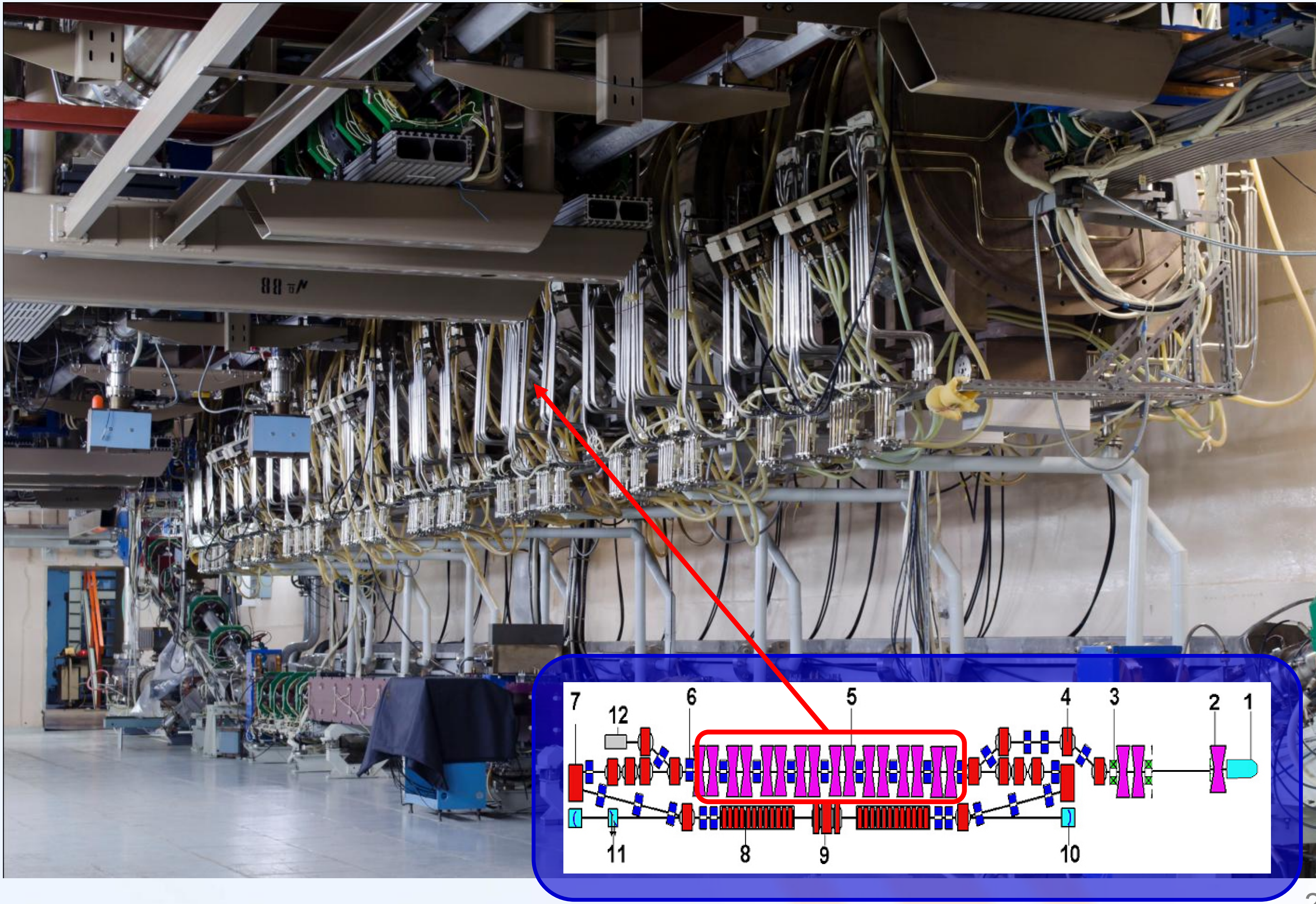

Main linac

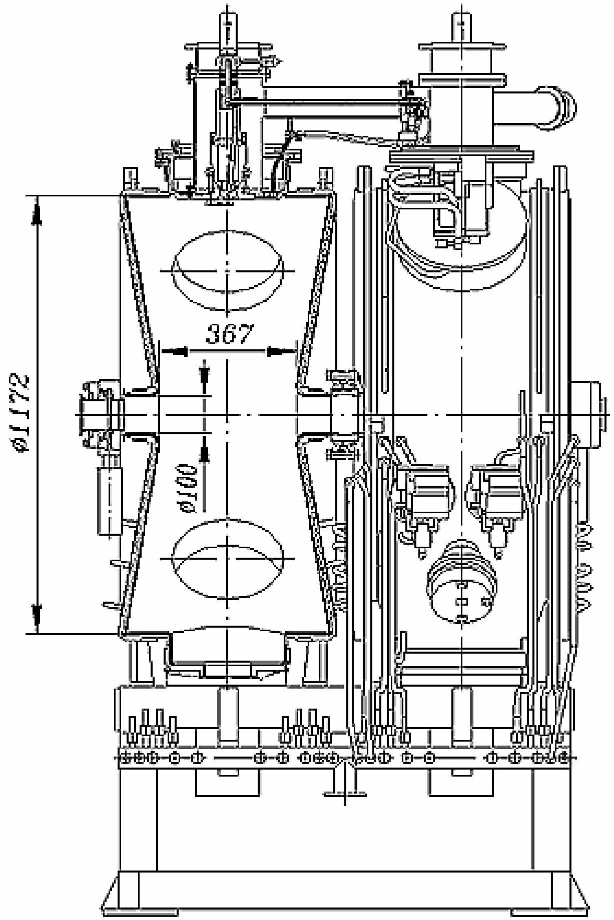

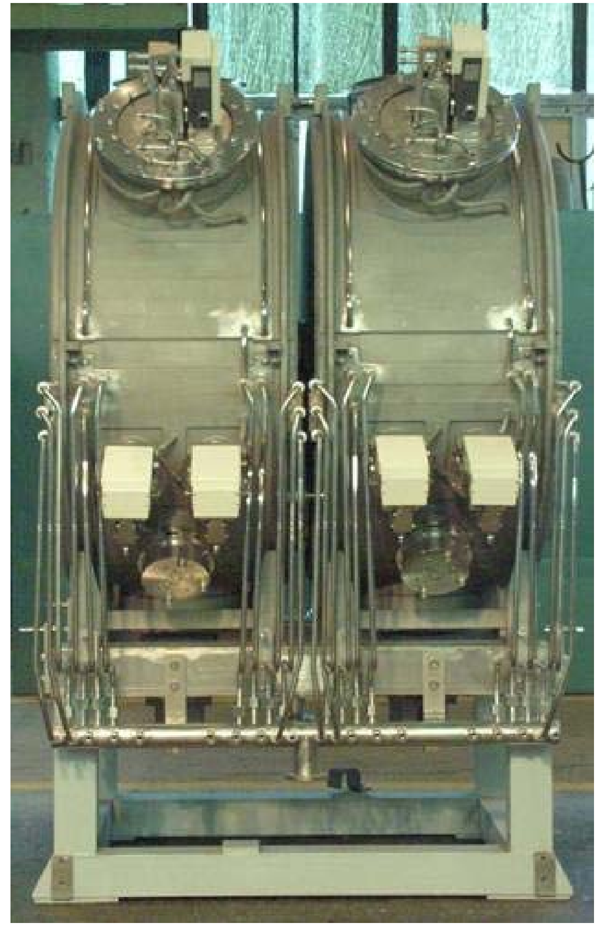

11
8
9
10
1

Undulator

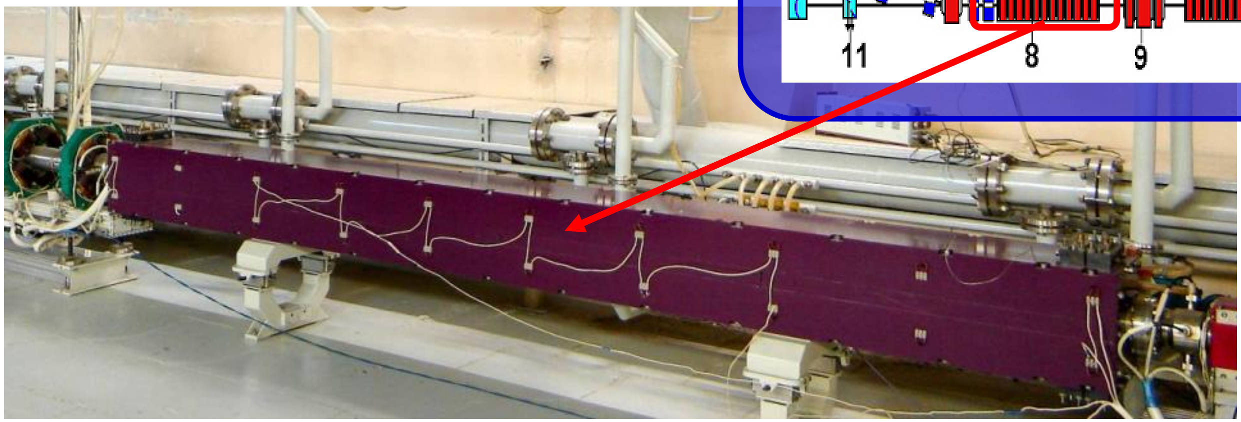

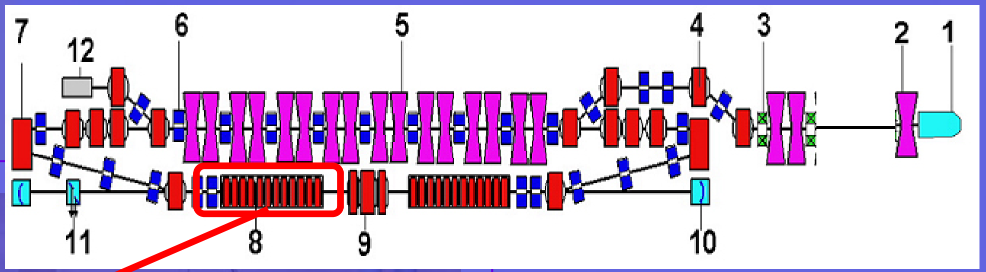

Period, cm	12
Maximum current, kA	2.4
Maximum K	1.25

Undulator

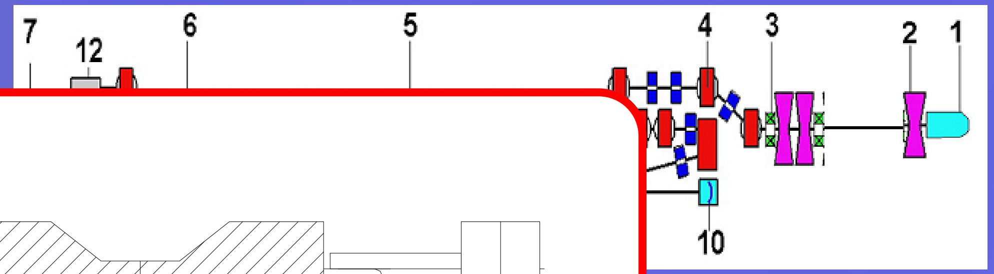

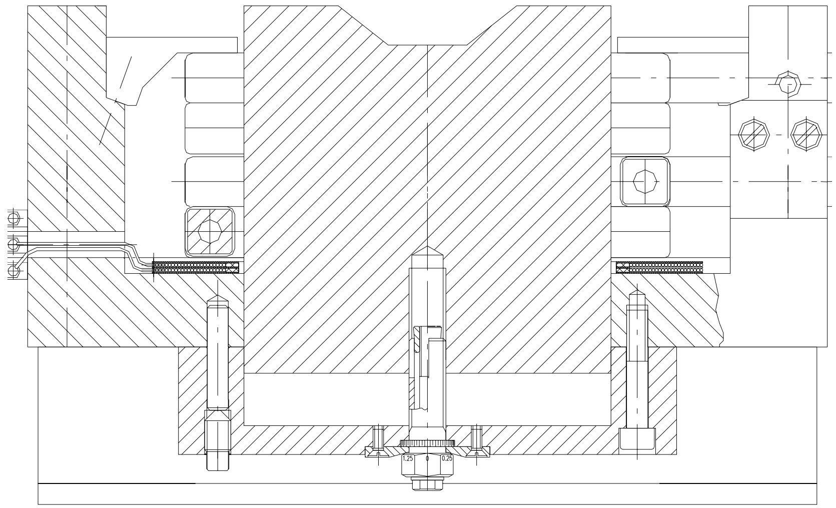

Maximum current, kA	2.4
Maximum K	1.25

Optical cavity

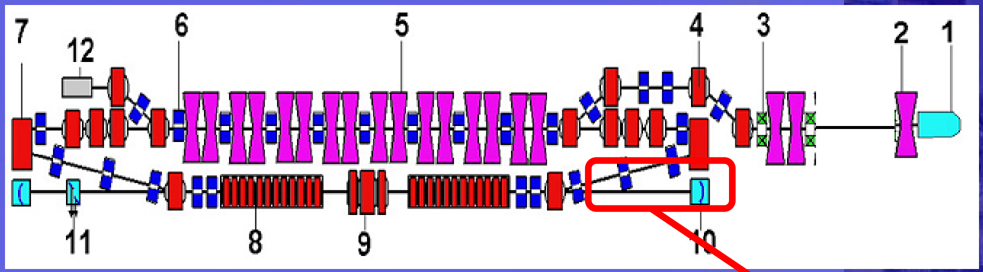

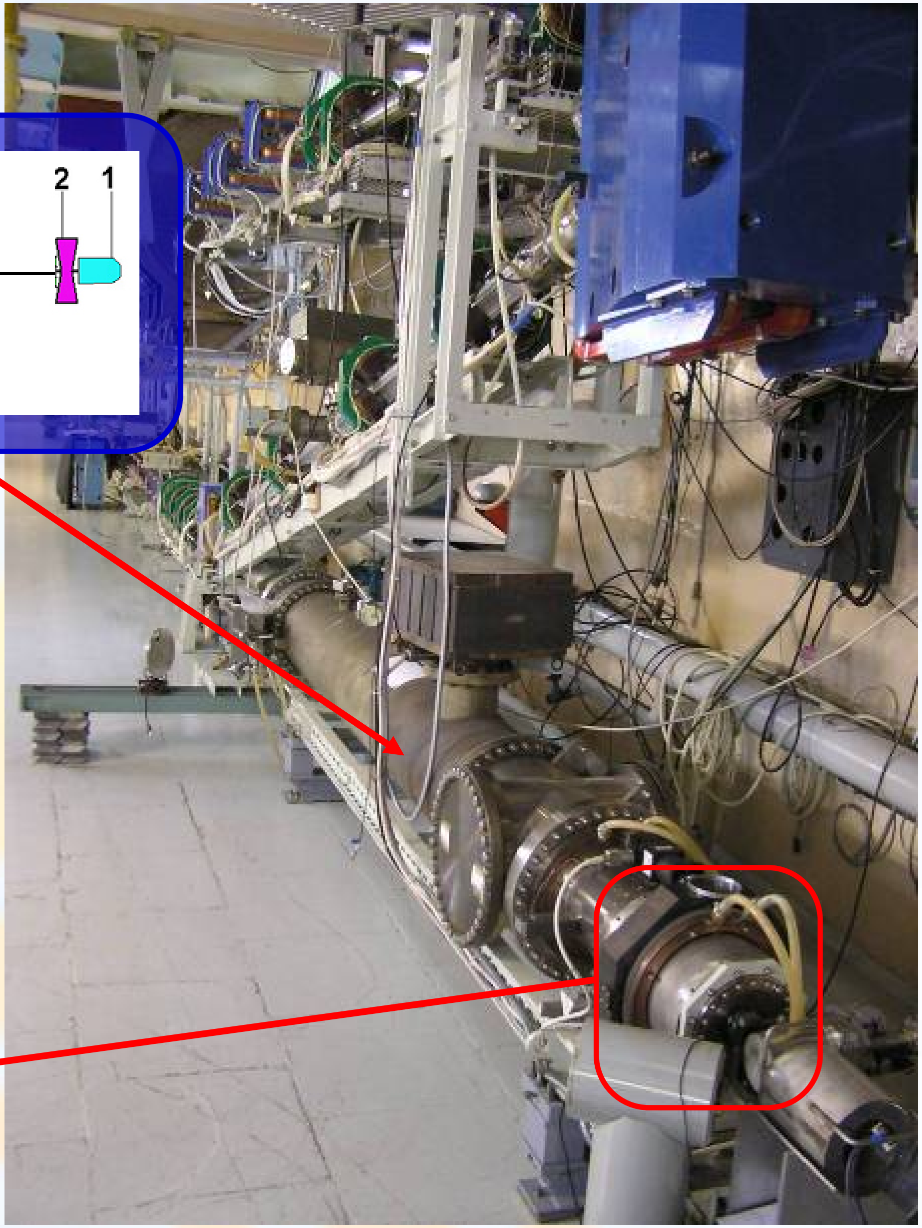

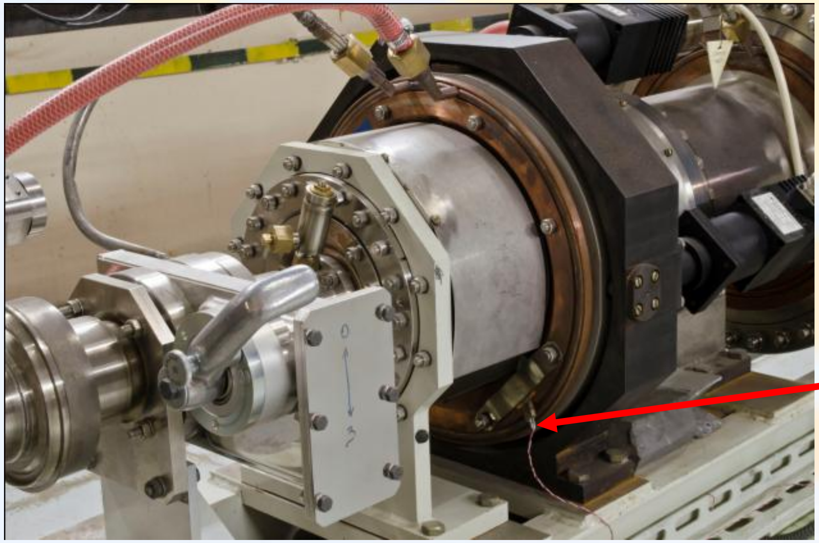

Radiation power time-dependence (1st stage)

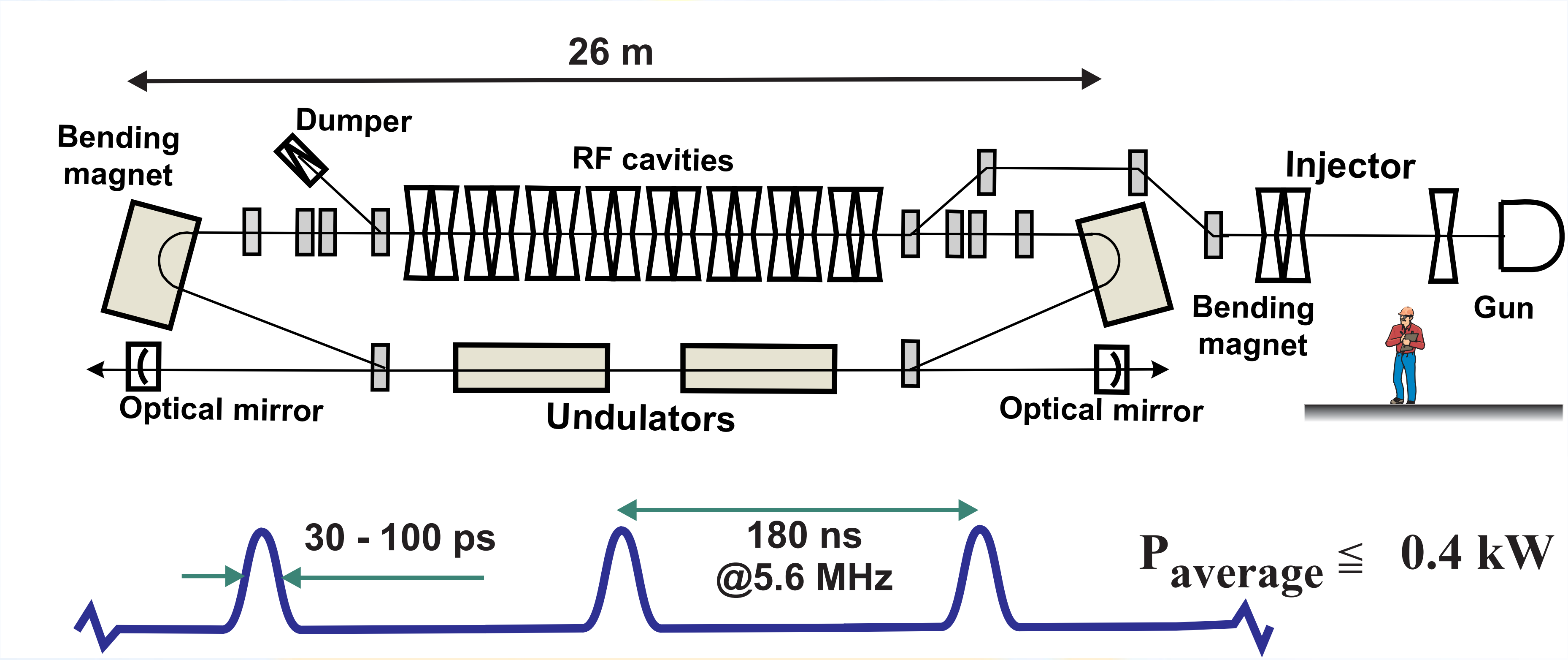

Optical beamline

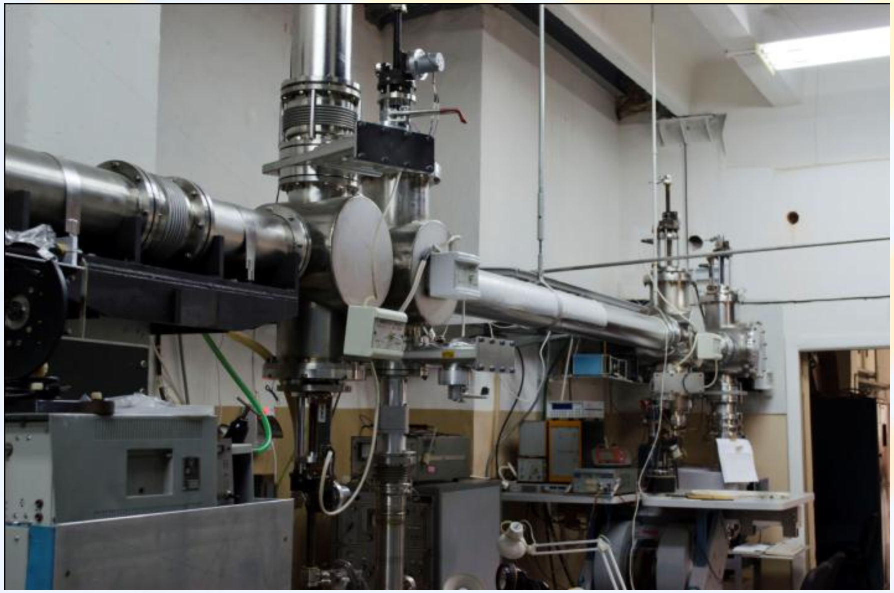

Optical beam expander

Optical beamline

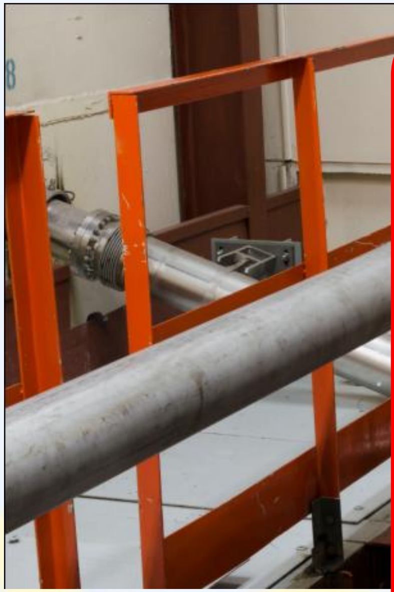

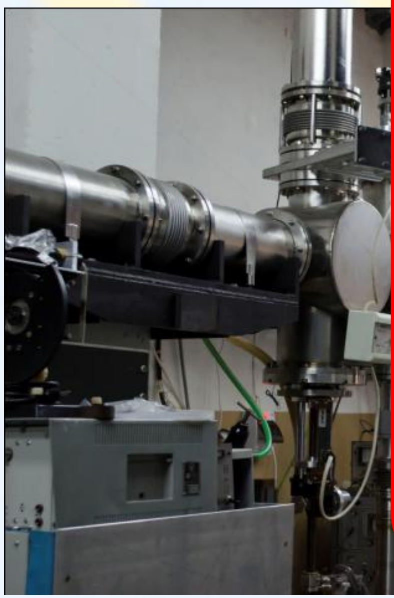

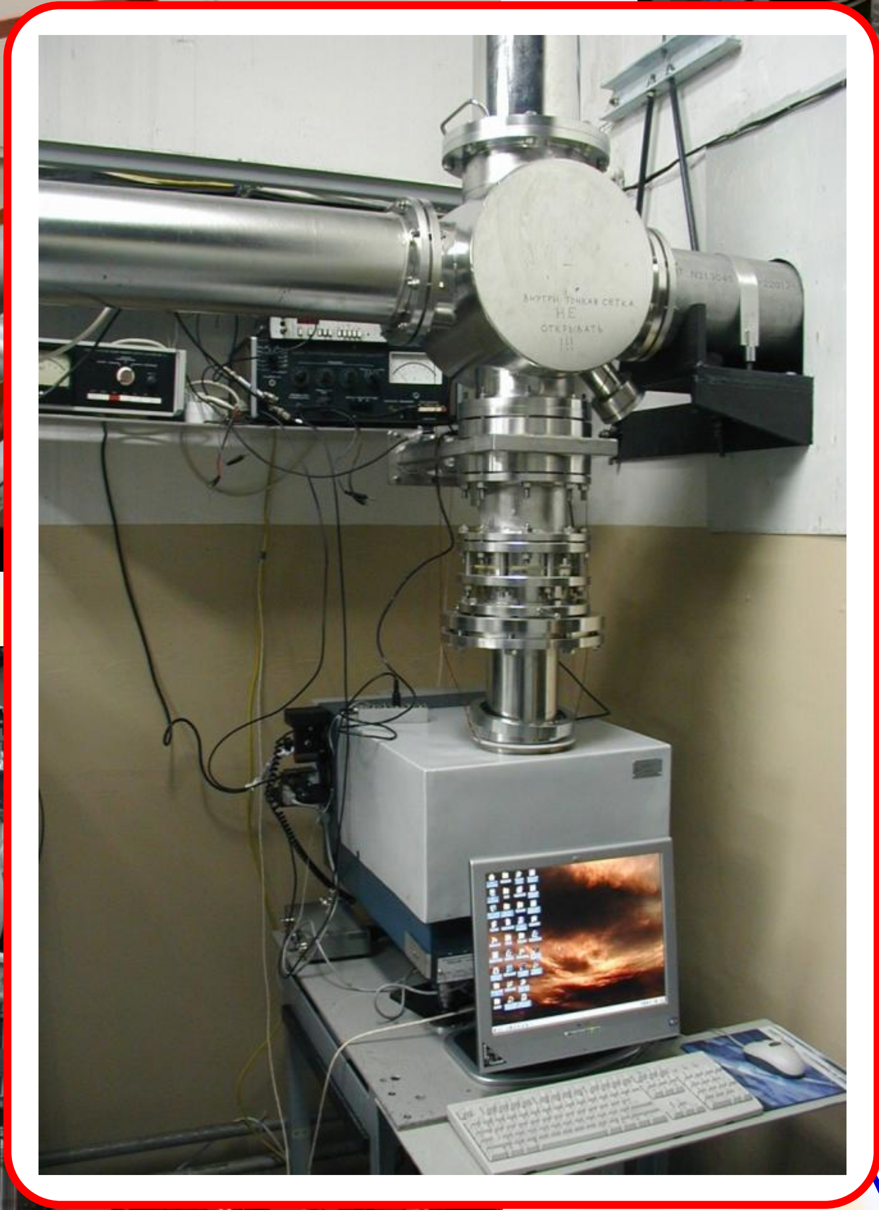

ical beam
xpander

Optical beamline

The 1st stage FEL radiation parameters

• Radiation wavelength, mm	0.12 - 0.24
• Pulse duration, ps	70
• Repetition rate , MHz	11.2
• Maximum average power, kW	0.5
• Minimum relative linewidth (FWHM)	$3 \cdot 10^{-3}$
• Peak power, MW	1

The obtained radiation parameters are still the world record in terahertz region.

Researches carried out at THz NovoFEL in 2011-2012

1. Measurement of molecular weight of synthetic polymers using THz ablation
2. Using THz ablation for study fractional composition of vaccines.
3. Study of the spectrum of electronic states in Si / CaF_2 BaF_2 / PbSnTe:In nanoheterostructures.
4. Investigation into the interaction of THz radiation with new functional resonant metamaterials for devices controlling the polarization, phase, intensity and direction of propagation of radiation.
5. Metamaterials based on precision micro- and nanoshells for terahertz and infrared ranges.
6. Investigation into the interaction of THz radiation with materials based on carbon nanotubes.
7. Production of carbon nanostructures with the help of NovoFEL radiation.
8. Determination of the fractional composition of nanoproducts of mechanical activation of double oxsides.
9. Exploration of composite silicon-polymer nanostructures.

Researches carried out at THz NovoFEL in 2011-2012

1. Measurement of molecular weight of synthetic polymers using THz ablation
2. Using THz ablation for study fractional composition of vaccines.
3. Study of the spectrum of electronic states in Si / CaF_2, BaF_2 / PbSnTe:In nanoheterostructures.
4. Investigation into the interaction of THz radiation with new functional resonant metamaterials for devices controlling the polarization, phase, intensity and direction of propagation of radiation.
5. Metamaterials based on precision micro- and nanoshells for terahertz and infrared ranges.
6. Investigation into the interaction of THz radiation with materials based on carbon nanotubes.
7. Production of carbon nanostructures with the help of NovoFEL radiation.
8. Determination of the fractional composition of nanoproducts of mechanical activation of double oxsides.
9. Exploration of composite silicon-polymer nanostructures.

- Pioneering works on THz ablation
- Study of micro- and nanoparticles, vaccines, polymers, metamaterials
- Production of nanotubes and nanostructures
- Composite diagnostics

Researches carried out at THz NovoFEL in 2011-2012

10.Spectral selective radioscopy.

11. Demonstration of imaging and detection of concealed objects.

12. Speckle photography and speckle interferometry.

13. Classic in-line holography.

14. Classic optical coherent tomography.

15. Talbot metrology.

16. Imaging attenuated total reflection (ATR) spectroscopy. Plasmon spectroscopy of surfaces and films.

17. Ellipsometry in THz region.

18. Development of methods for flame diagnostics using the THz FEL.

19. Investigation of H_2-O_2 combustion by THz radiation tuned on H_2O absorbing lines.

20. Measurements of the concentration of H_2O vapor in flames.

21. Investigation of the explosion and detonation in gas mixtures.

Researches carried out at THz NovoFEL in 2011-2012

- Terahertz radioscopy, imaging, detection of concealed objects
- Interferomety, holography & tomography
- Speckle and Talbot metrology
- Ellipsometry
- Fast water vapor detection
- Flame and gas detonation study

10. Spectral selective radioscopy.
11. Demonstration of imaging and detection of concealed objects.
12. Speckle photography and speckle interferometry.
13. Classic in-line holography.
14. Classic optical coherent tomography.
15. Talbot metrology.
16. Imaging attenuated total reflection (ATR) spectroscopy. Plasmon spectroscopy of surfaces and films.
17. Ellipsometry in THz region.
18. Development of methods for flame diagnostics using the THz FEL.
19. Investigation of H_2-O_2 combustion by THz radiation tuned on H_2O absorbing lines.
20. Measurements of the concentration of H_2O vapor in flames.
21. Investigation of the explosion and detonation in gas mixtures.

Researches carried out at THz NovoFEL in 2011-2012

22. Study of the impact of THz radiation on genetic material.
23. Exploration of the impact of THz radiation on stress-sensitive biological cell systems.
24. THz radiation influence of the katG and E.coli dps genes.
25. Study of the integrated proteomic response of E.coli to exposure by terahertz radiation.
26. Exploration of coherent effects in gas in experiments using THz free electron laser.
27. Ultrafast high-resolution THz time-domain spectroscopy.
28. Experimental study of photoeffect for noble gas atoms in strong terahertz field.

Researches carried out at THz NovoFEL in 2011-2012

22. Study of the impact of THz radiation on genetic material.
23. Exploration of the impact of THz radiation on stress-sensitive biological cell systems.
24. THz radiation influence of the katG and E.coli dps genes.
25. Study of the integrated proteomic response of E.coli to exposure by terahertz radiation.
26. Exploration of coherent effects in gas in experiments using THz free electron laser.
27. Ultrafast high-resolution THz time-domain spectroscopy.
28. Experimental study of photoeffect for noble gas atoms in strong terahertz field.

- Impact of THz radiation on genetic materials
- Impact of THz radiation on cells
- Study of integrated proteomic response
- Coherent effects in gases
- Ultrafast time-domain spectroscopy
- Interaction atoms with strong THz EM-field

Second and third stages beamlines

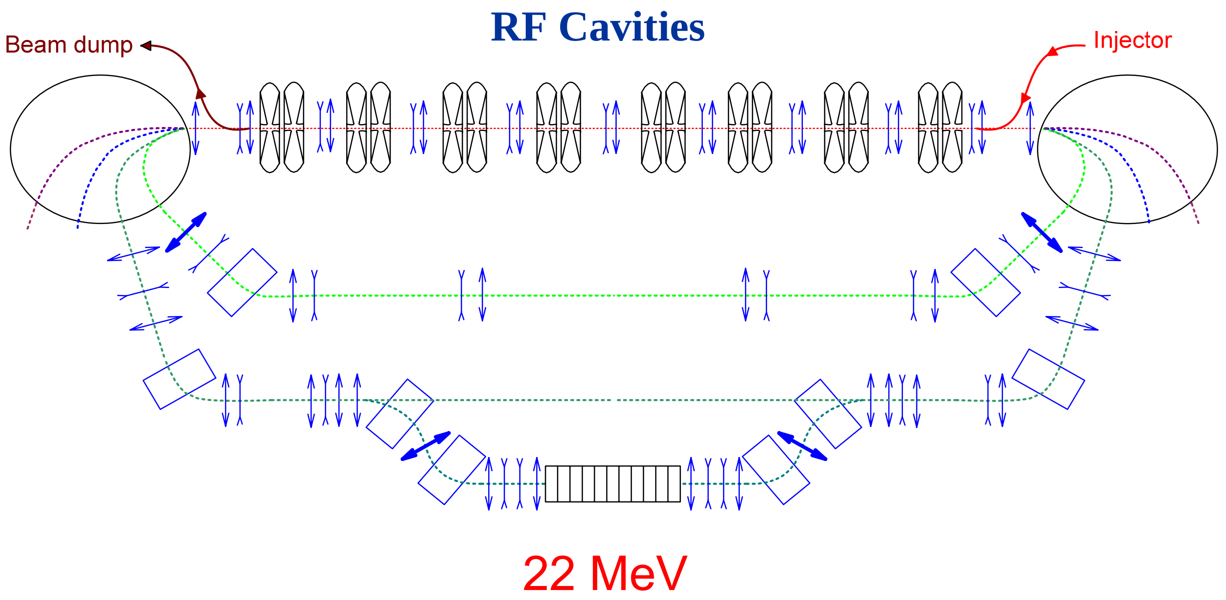

(horizontal plane)

Second and third stages beamlines

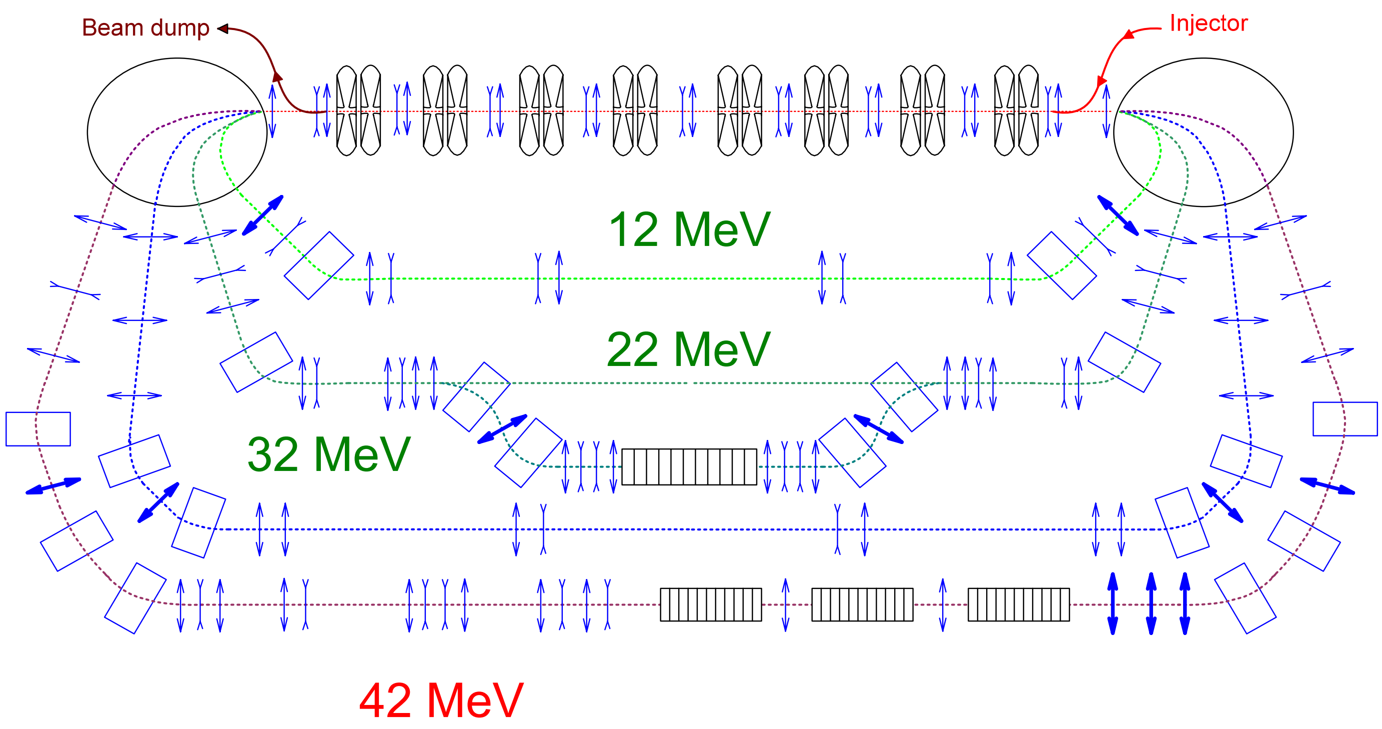

(horizontal plane)

Magnets and vacuum chamber of bends

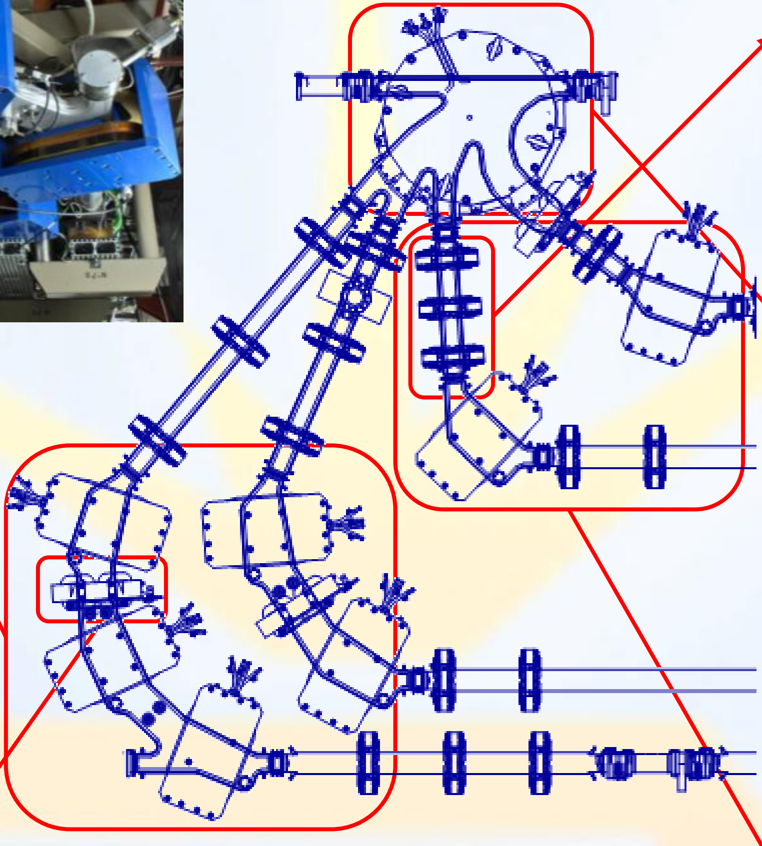

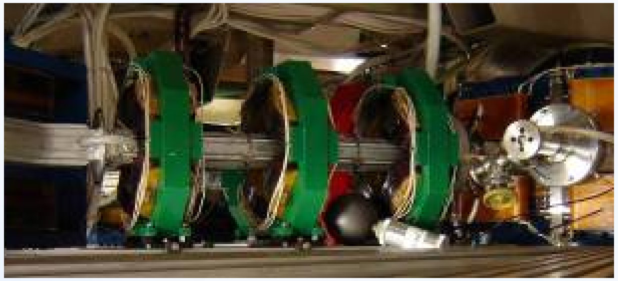

Quadrupole gradient distribution

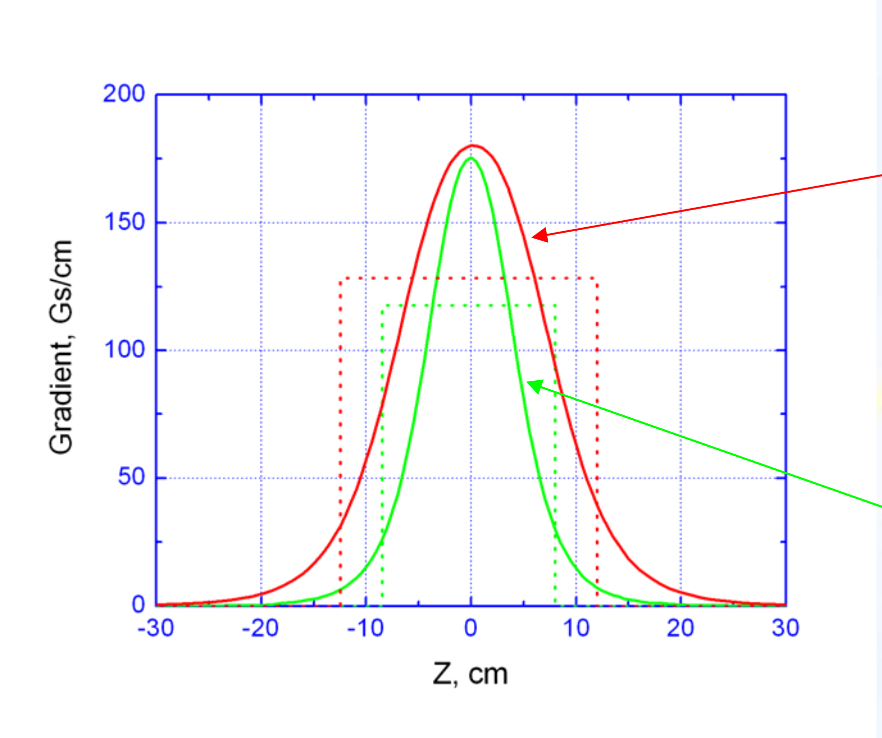

I = 250 A

I = 10 A

Representation of real quadrupole with ideal one

$$L_{eff} = \frac{6}{I_0^2} \int_{-\infty}^{\infty} \left(\int_{-\infty}^{z} g(z')dz' \cdot \left(I_0 - \int_{-\infty}^{z} g(z')dz' \right) \right) dz \qquad g_{eff} = \frac{I_0}{L_{eff}}$$

$$x'' + g(z)x = 0$$

$$I_0 = \int_{-\infty}^{\infty} g(z)dz$$

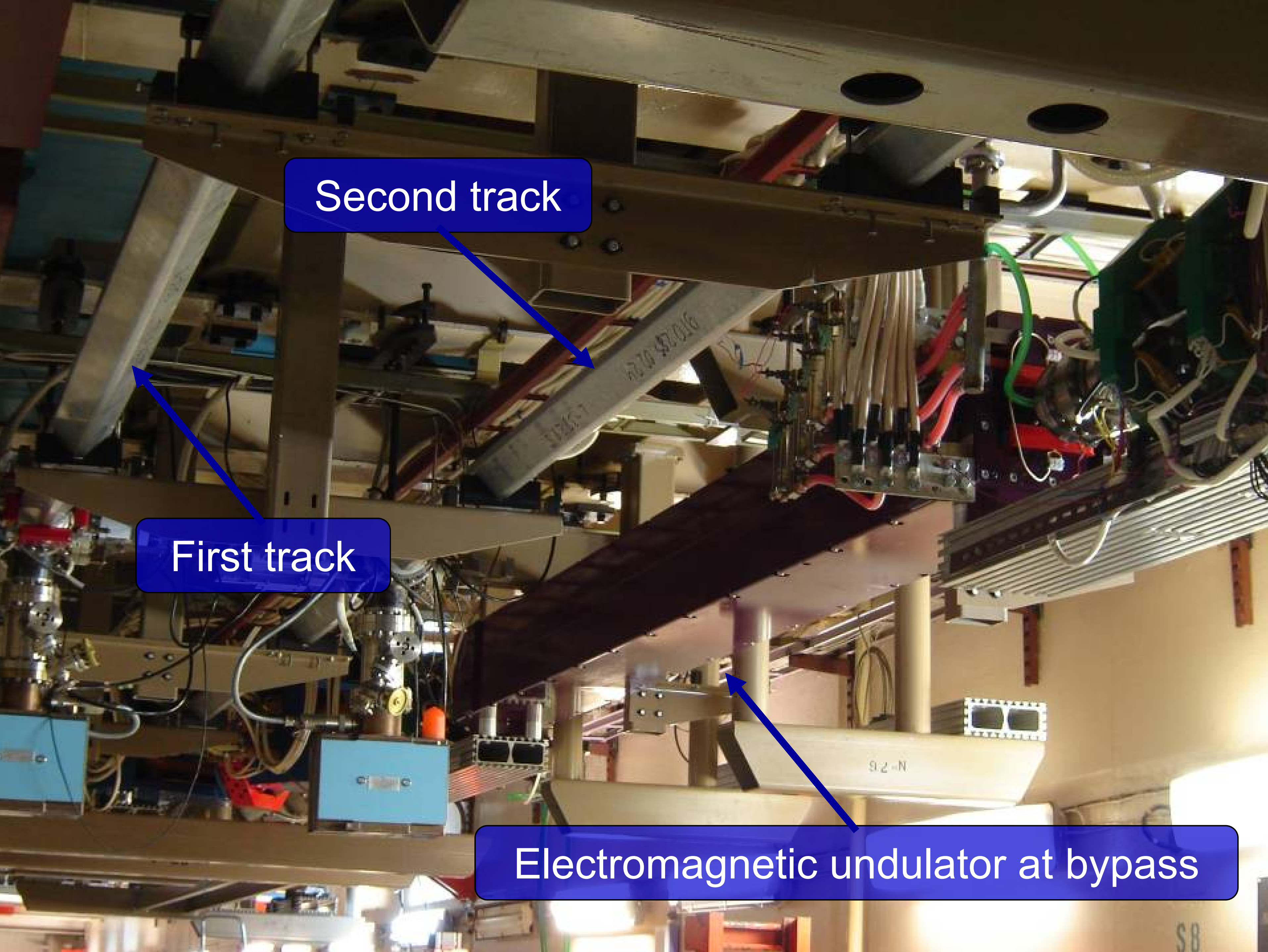
Second track
First track
Electromagnetic undulator at bypass

Optimization of the energy acceptance

Before FEL

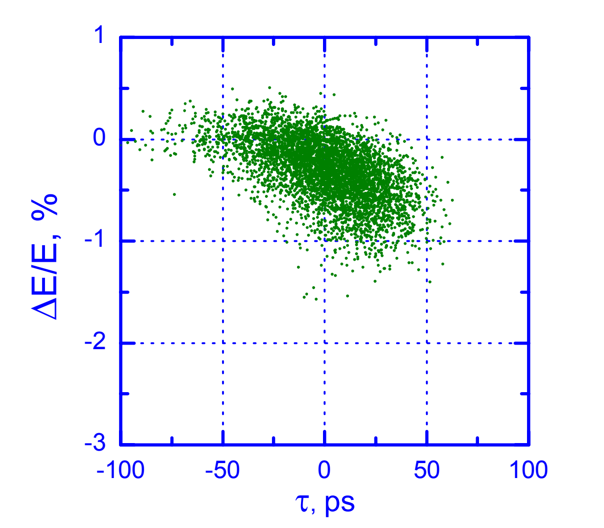

After FEL

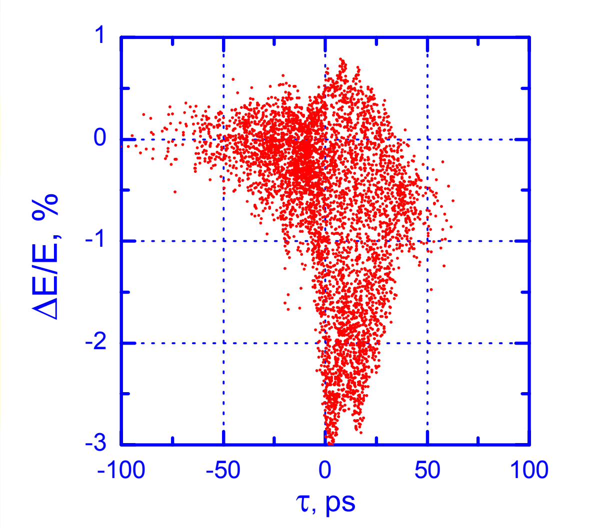

Interaction of electrons with radiation in FEL leads to large energy spread. Moreover the relative energy spread increases at deceleration. Therefore the longitudinal acceptance is very important parameter of ERLs which work for FELs

Optimization of the energy acceptance

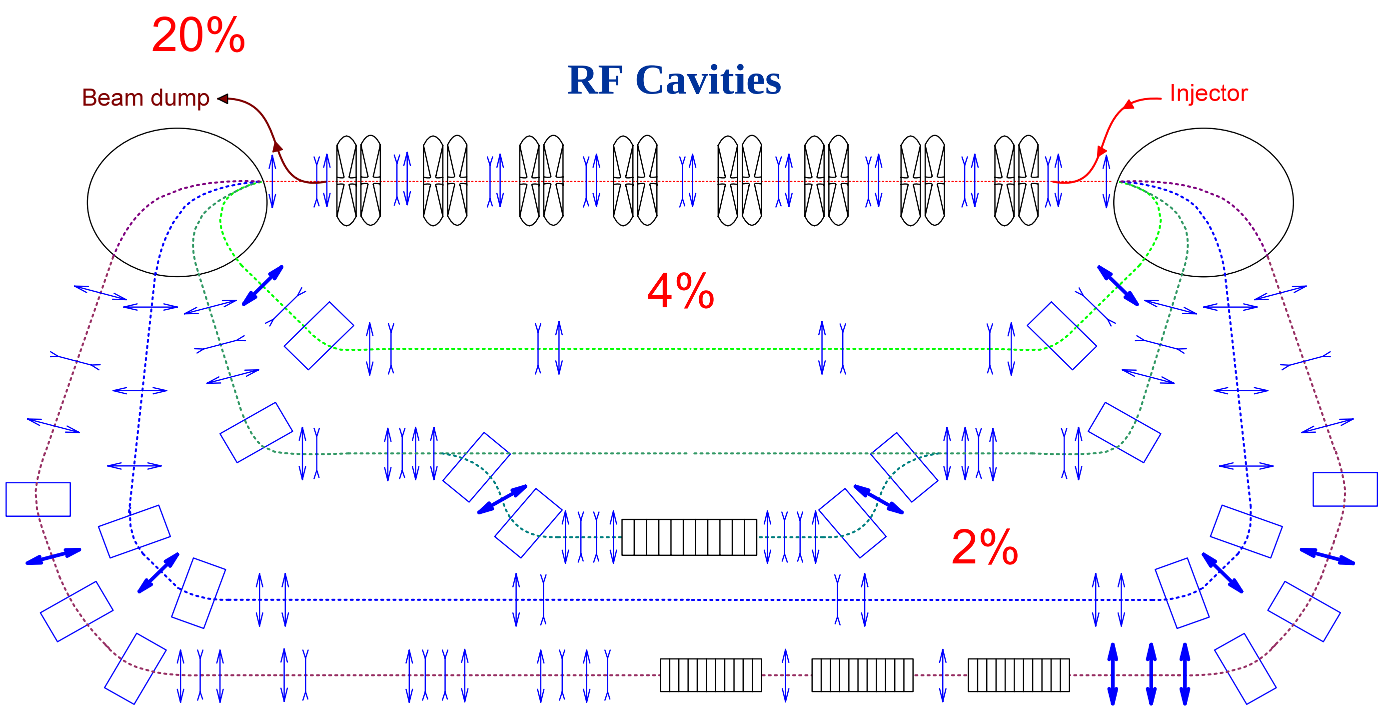

1. Compensation of chromatic aberrations

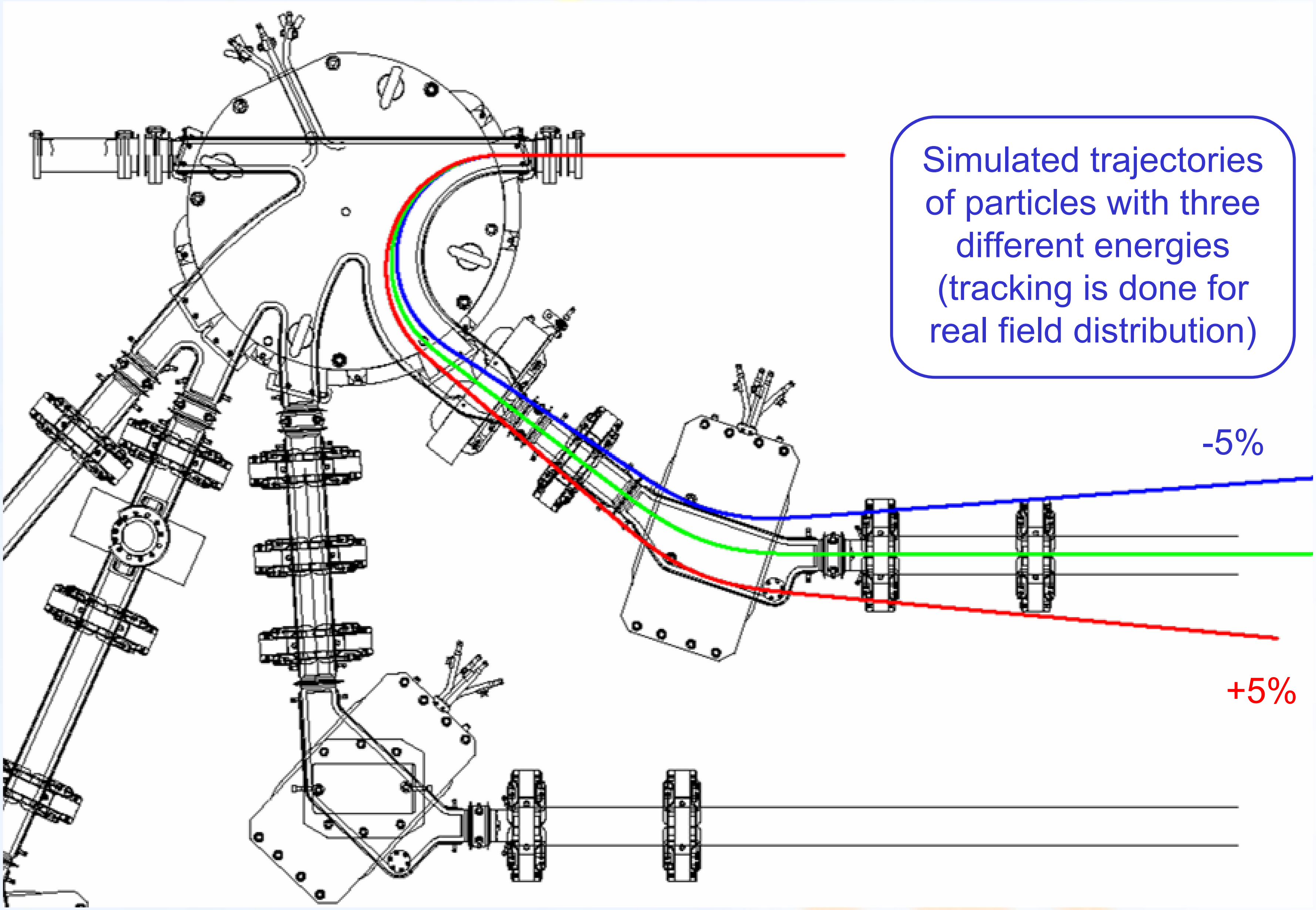

Simulated trajectories of particles with three different energies (tracking is done for real field distribution)

1. Compensation of chromatic aberrations

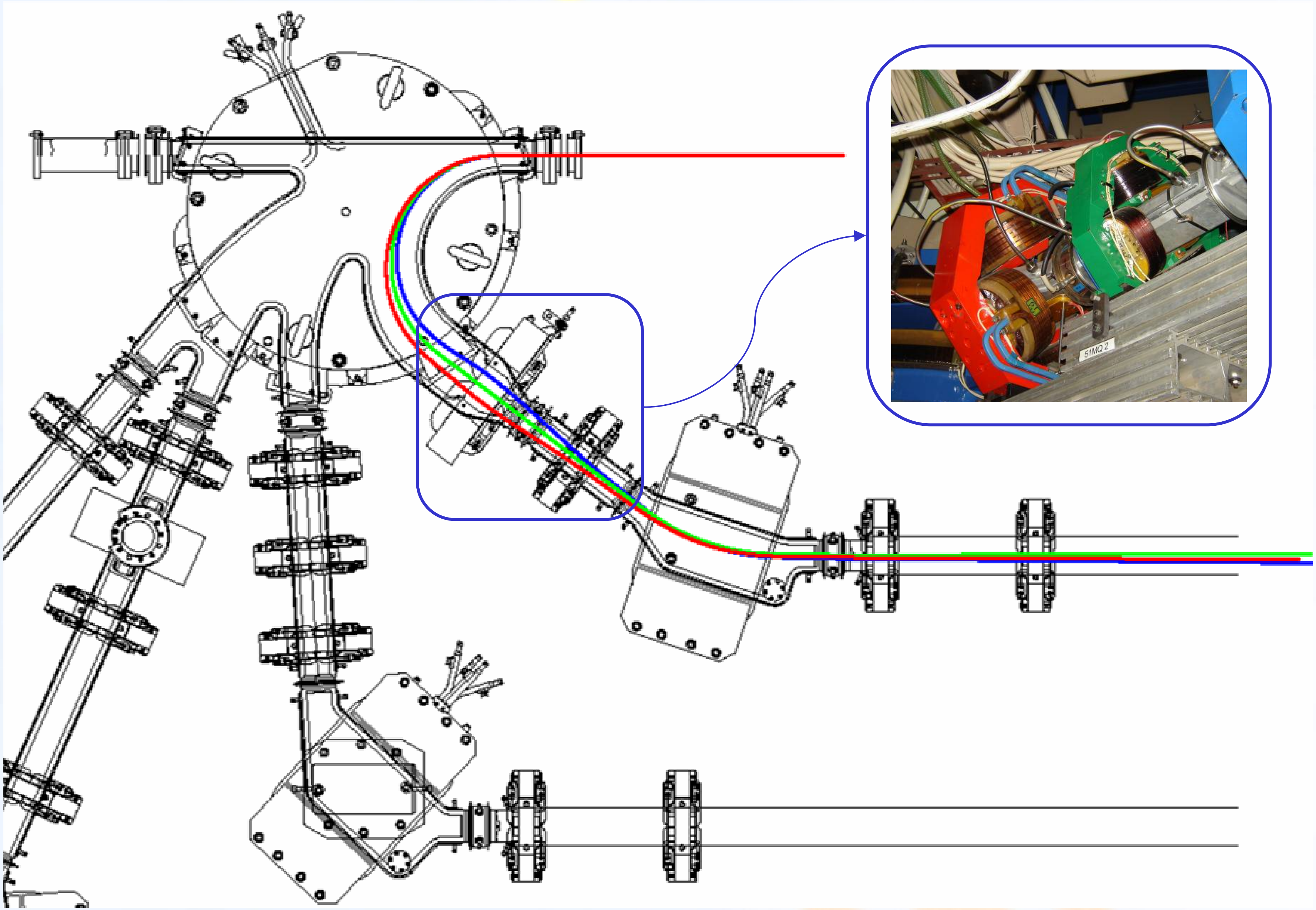

1. Compensation of chromatic aberrations

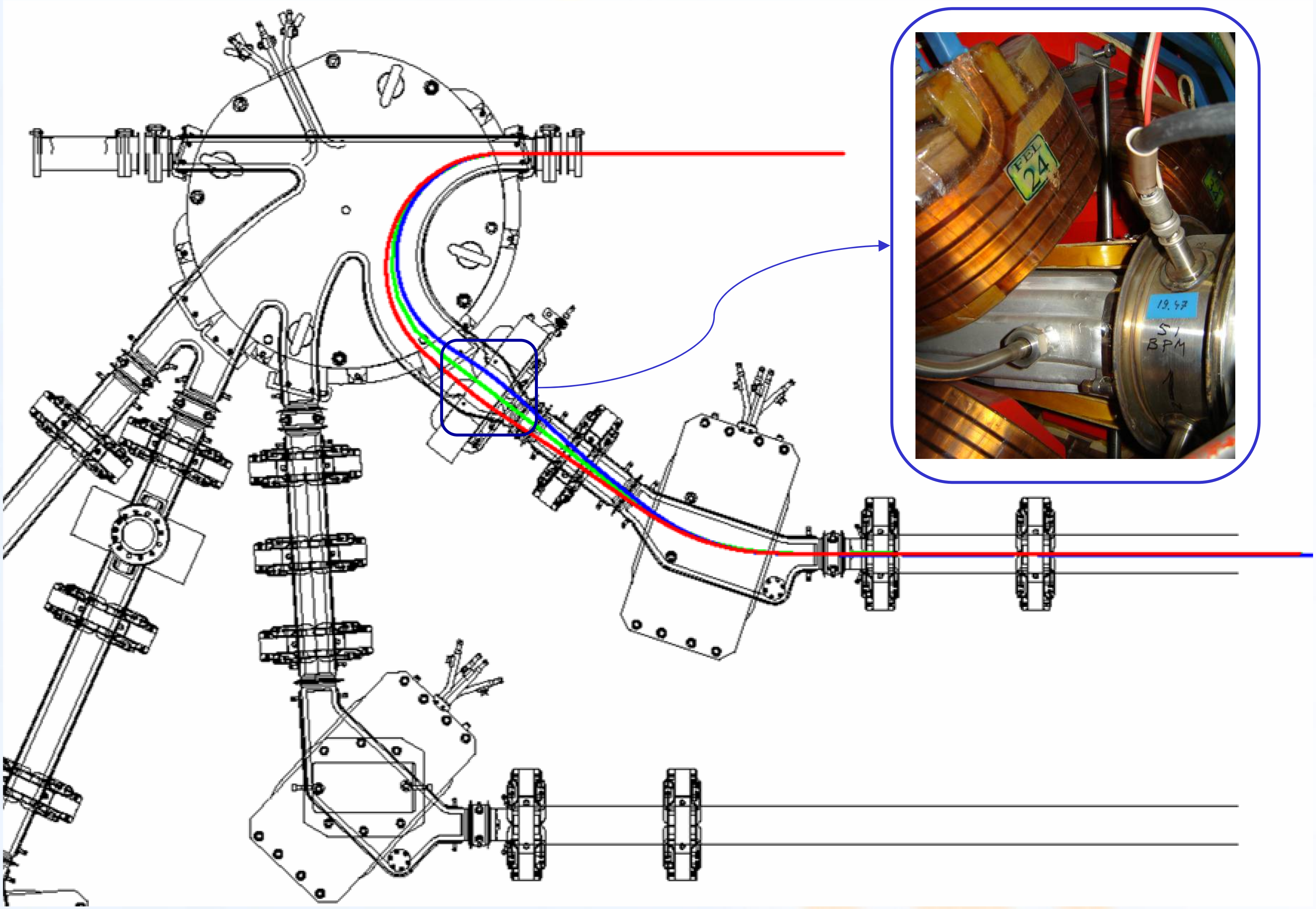

1. Compensation of chromatic aberrations

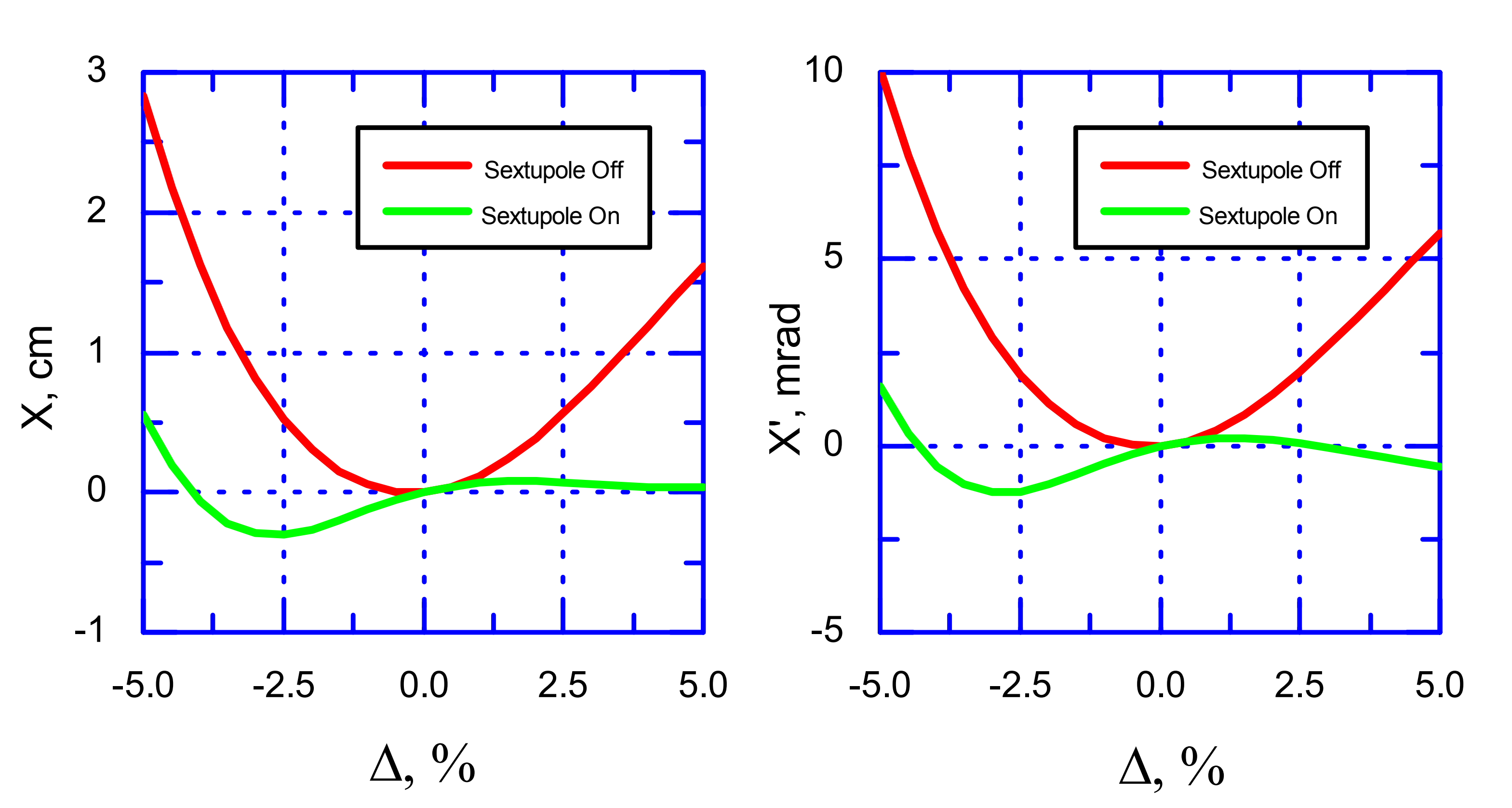

$$\delta\varepsilon = \frac{1}{2\varepsilon_0}\left(\beta_0\left\langle X'(\Delta)^2\right\rangle + 2\alpha_0\left\langle X'(\Delta)X(\Delta)\right\rangle + \gamma_0\left\langle X(\Delta)^2\right\rangle\right)$$

Emittance degradation

2. Optimization of the deceleration phase

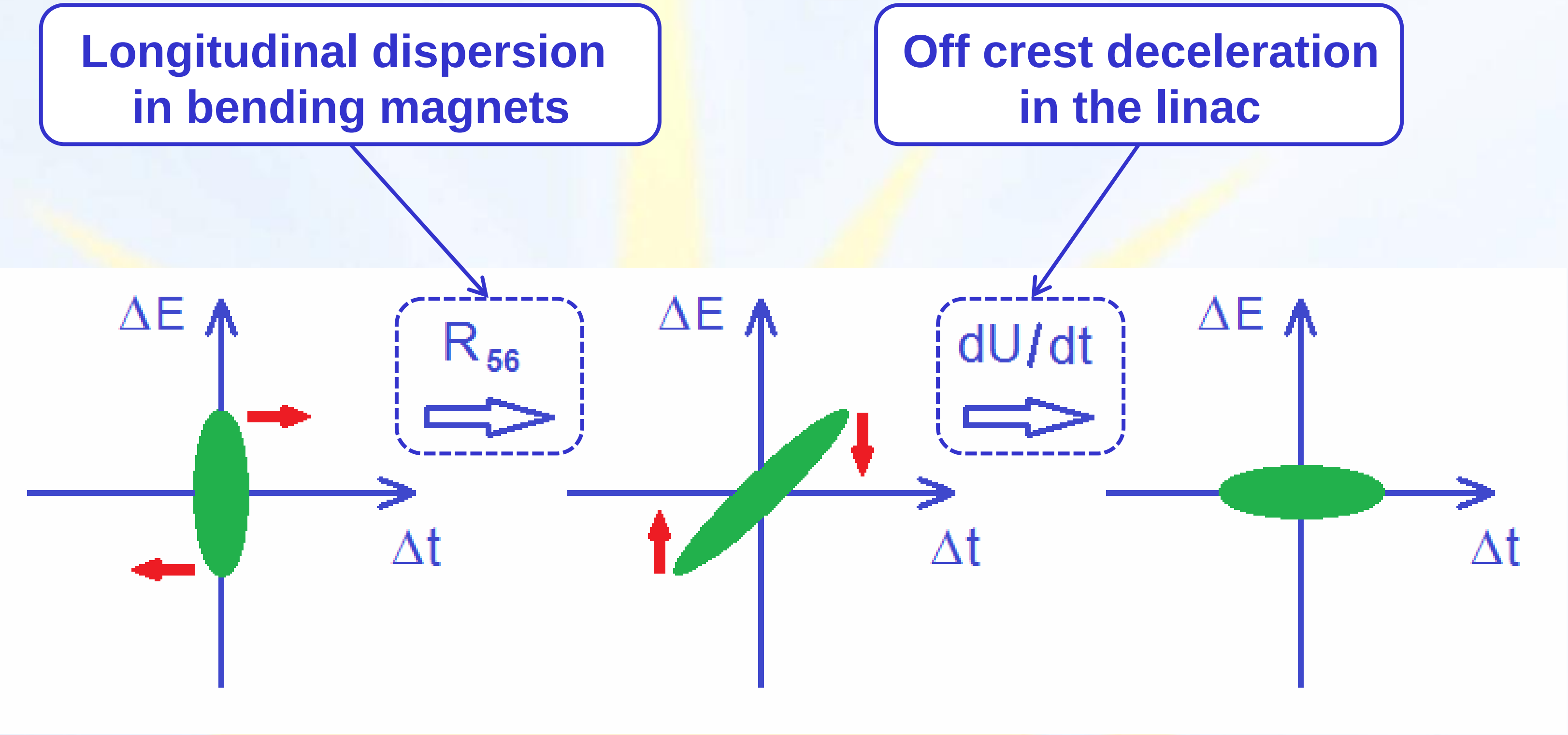

2. Optimization of the deceleration phase

The first track

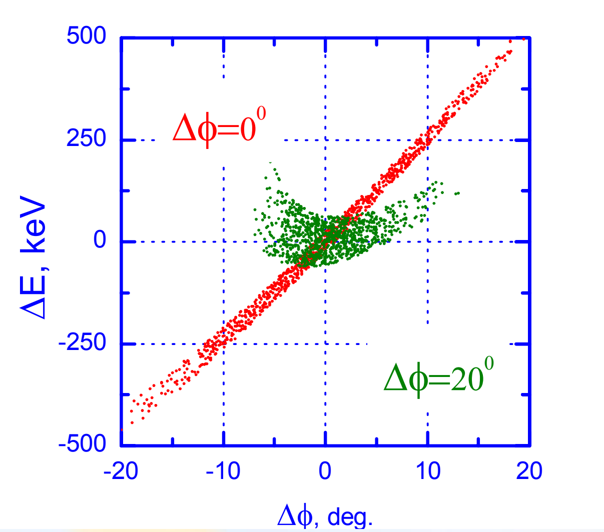

The dump

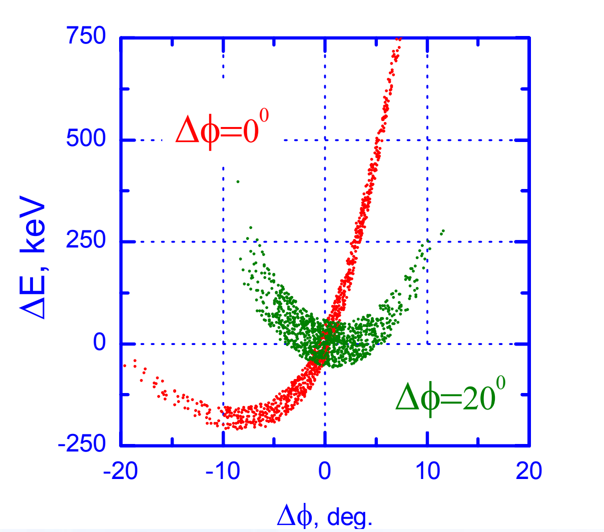

Beam longitudinal phase space for different deceleration phases

2. Optimization of the deceleration phase

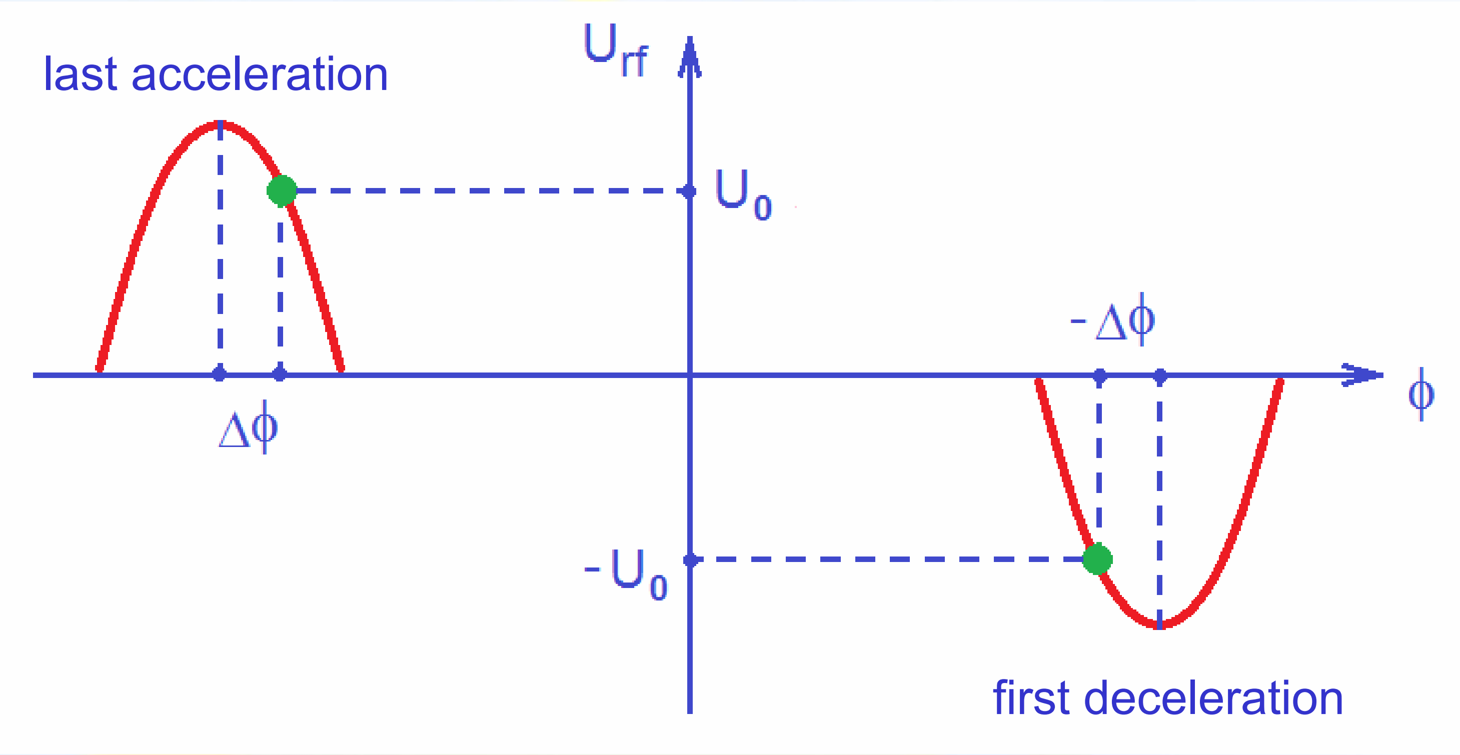

$$L = \lambda_{rf}\left(N + \frac{1}{2} - \frac{\Delta\varphi}{\pi}\right)$$

Length of the last track

Adjustment of the orbit length

Common track round magnet

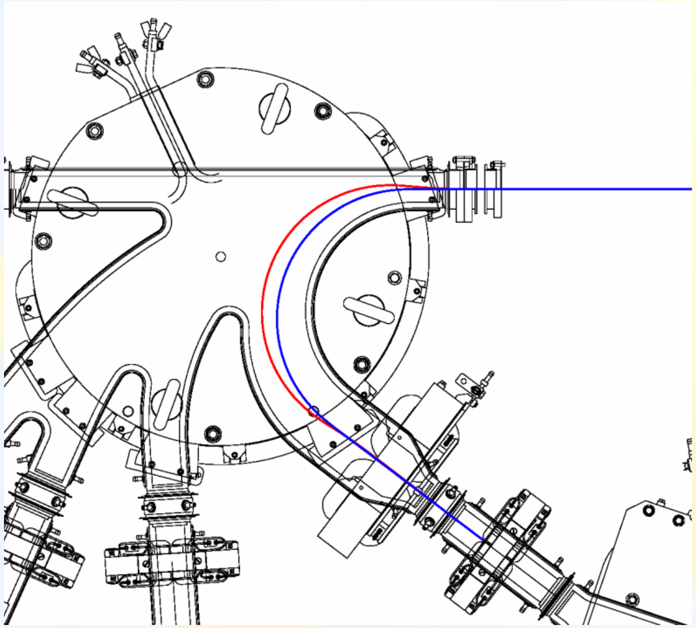

ΔL = 8 cm

Second track bending magnet

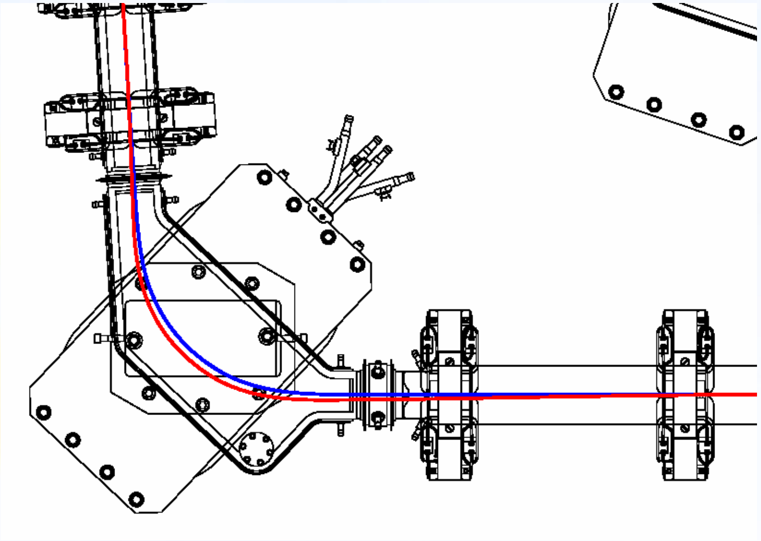

ΔL = 2 cm

Adjustment of the longitudinal dispersion
(after bypass)

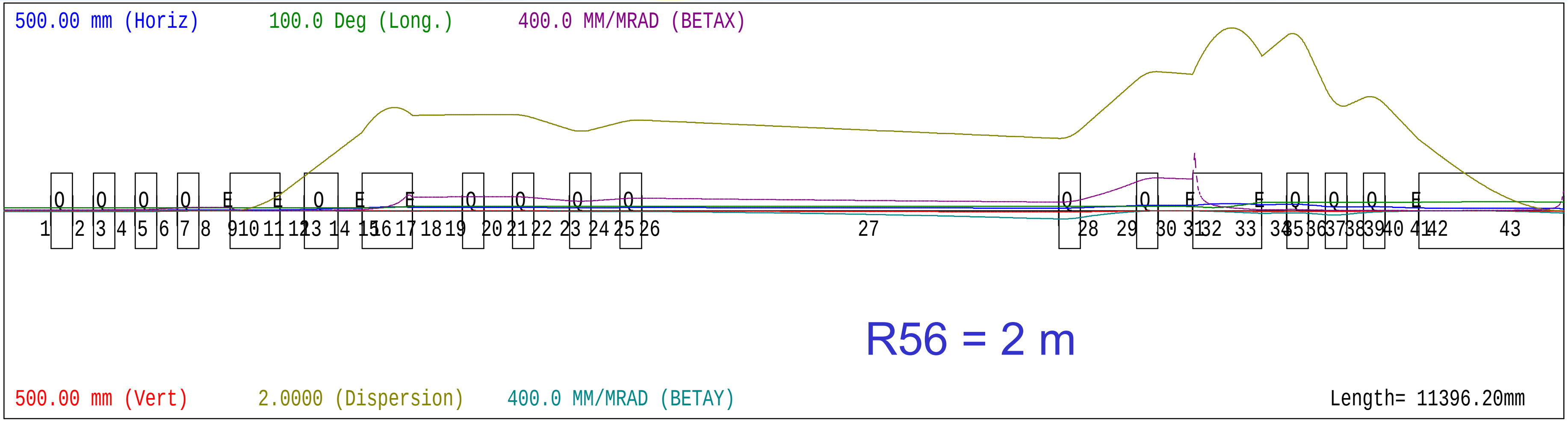

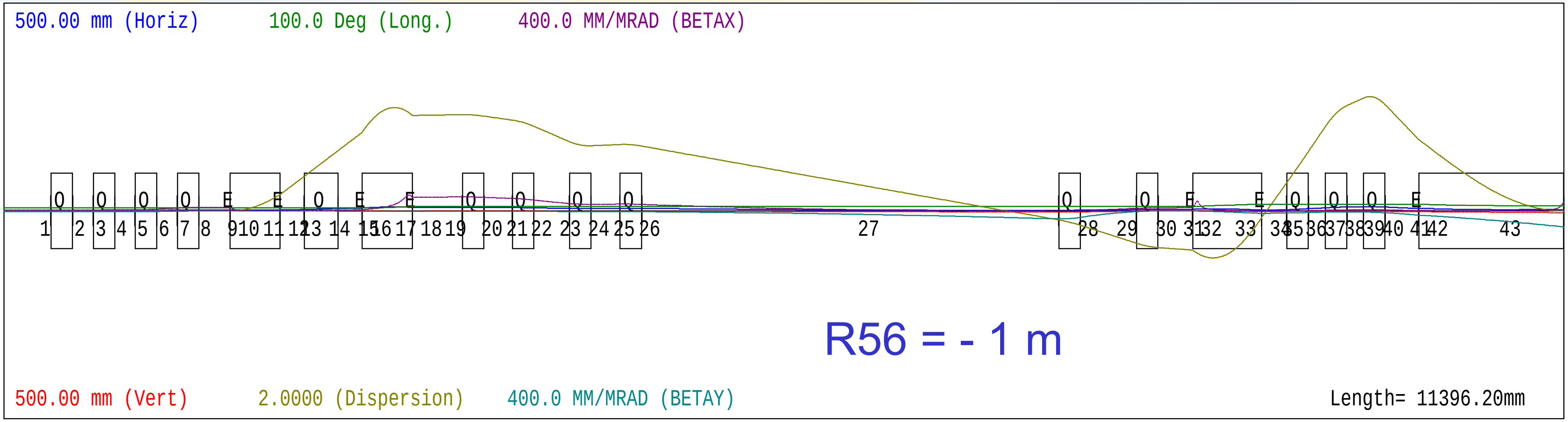

Second and third stages beamlines

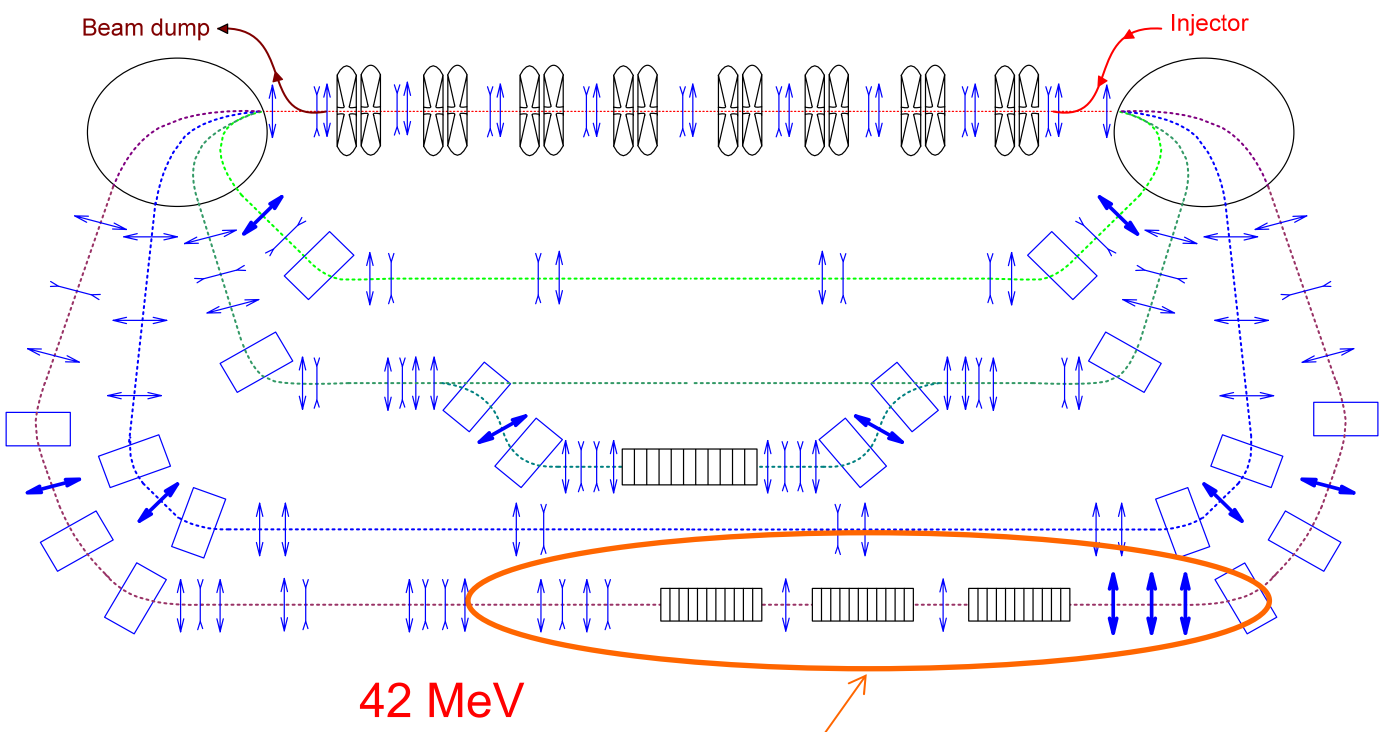

Electron outcoupling scheme is used here

Second and third stages beamlines

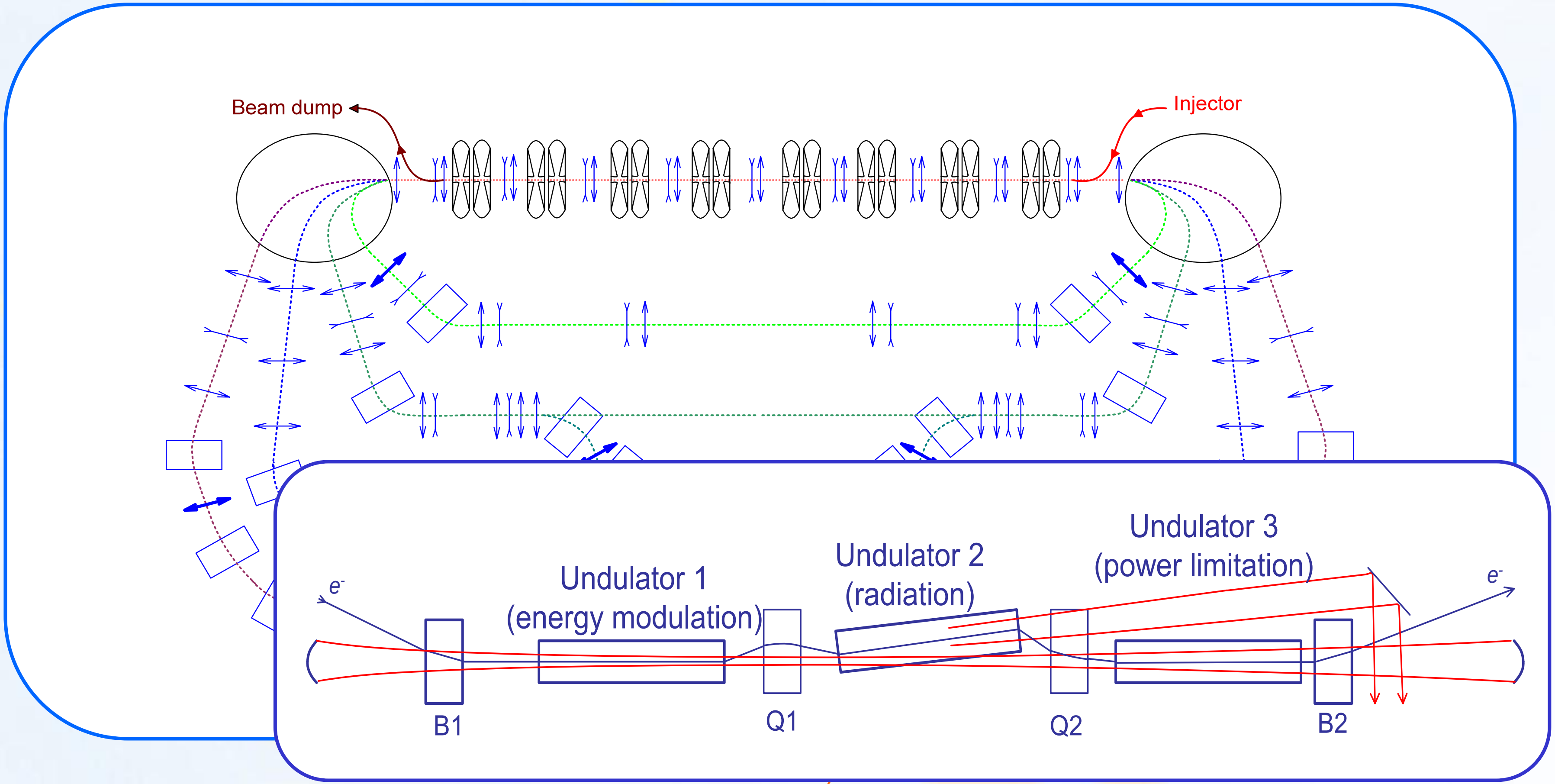

Electron outcoupling scheme is used here

The 3^{rd} stage FEL undulator

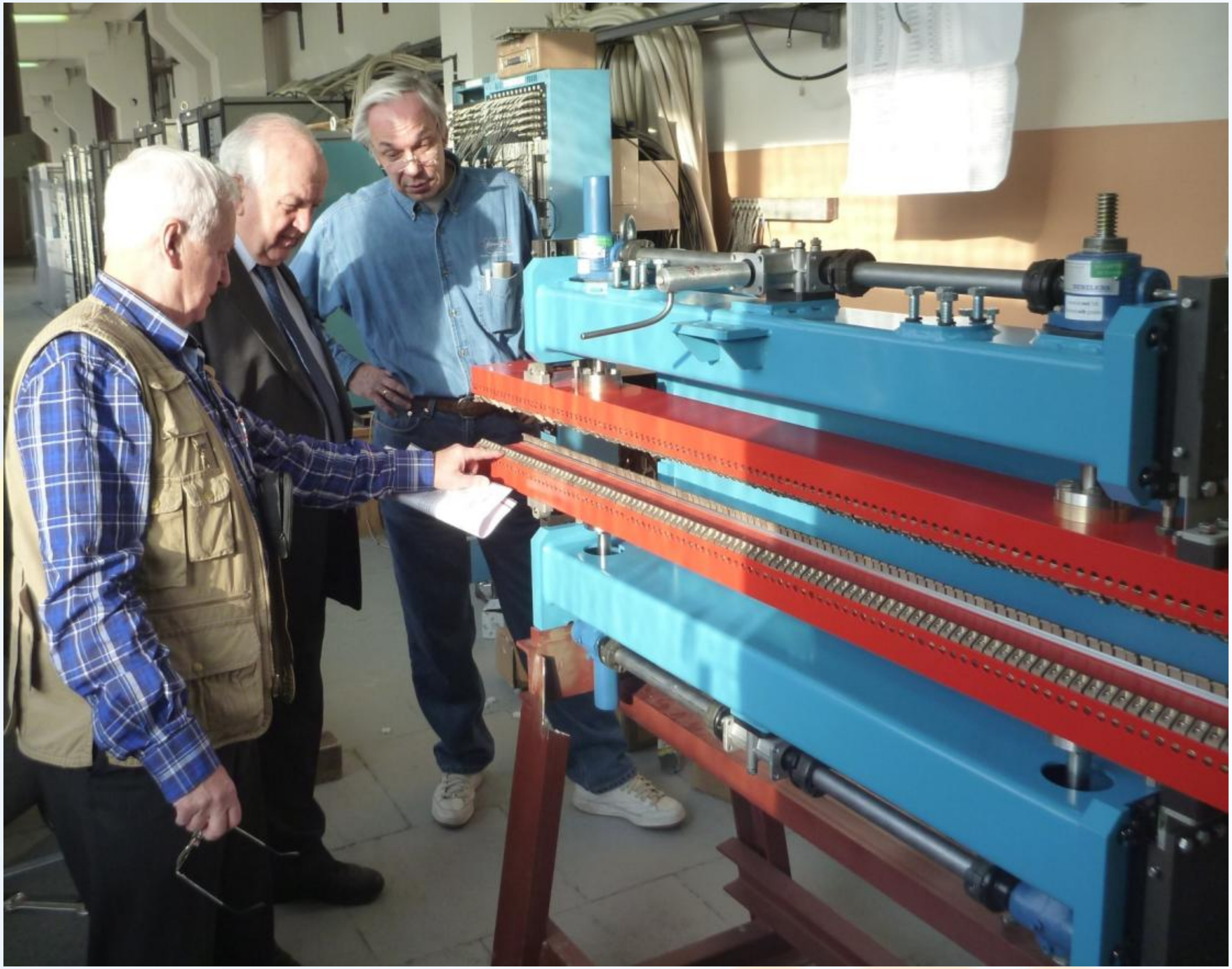

The 3rd stage FEL undulator

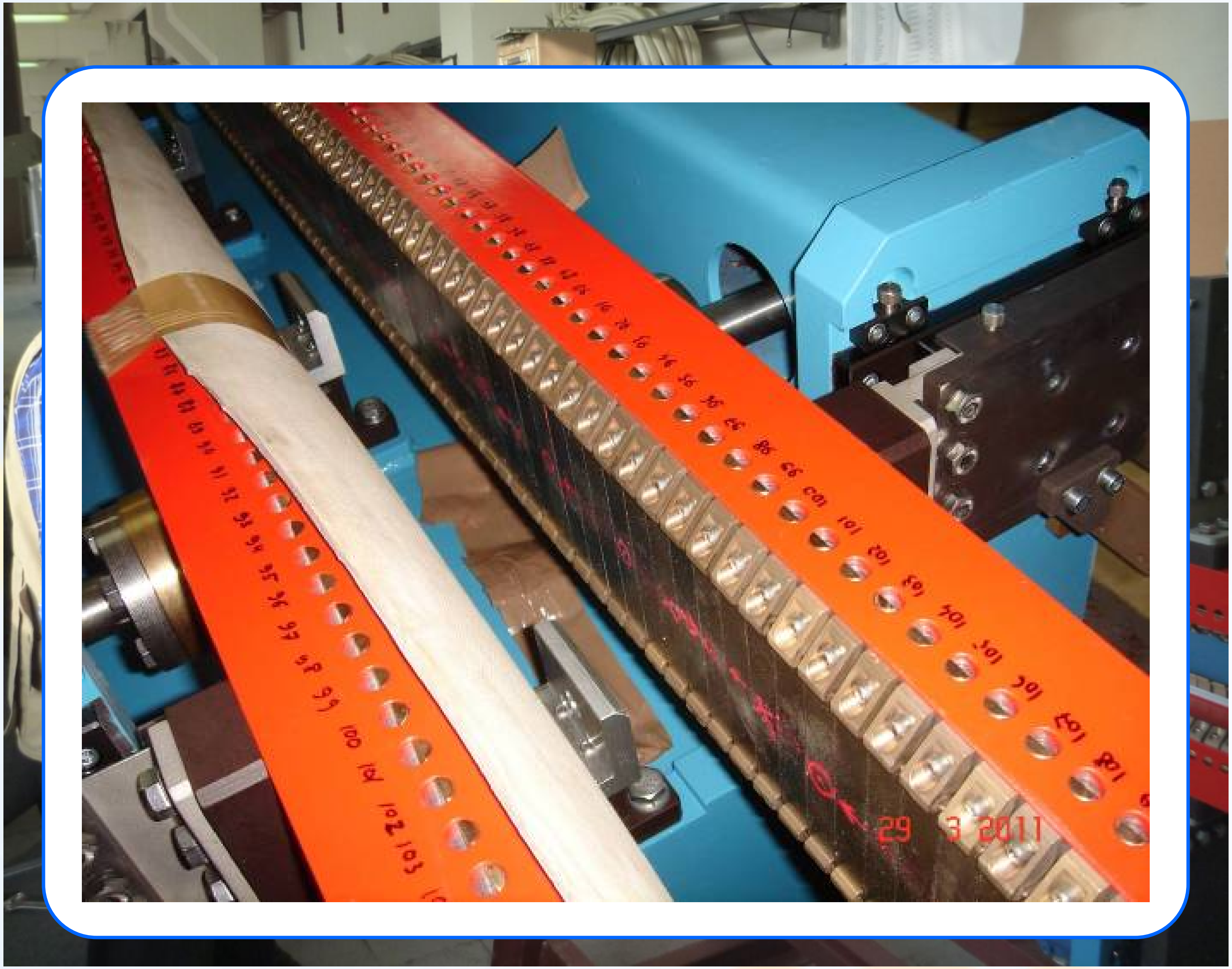

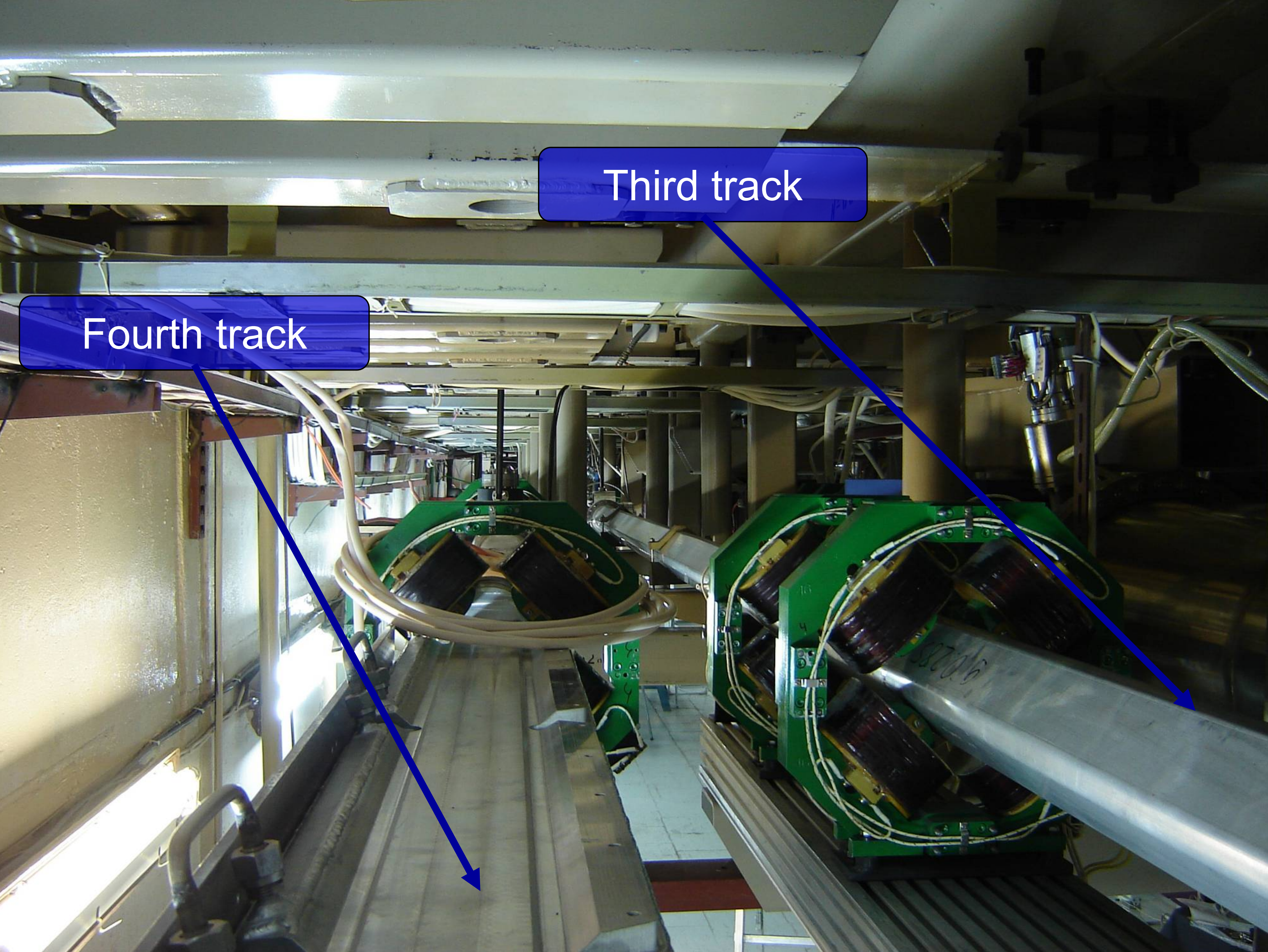
Third track
Fourth track

The second and the third stages ERL and FEL basic parameters

Electron beam energy, MeV	20/40
Number of orbits	2/4
Maximum bunch repetition frequency, MHz	22 (90)
Beam average current, mA	30 (100)
Wavelength range, micron	5-120
Maximum output power, kW	10

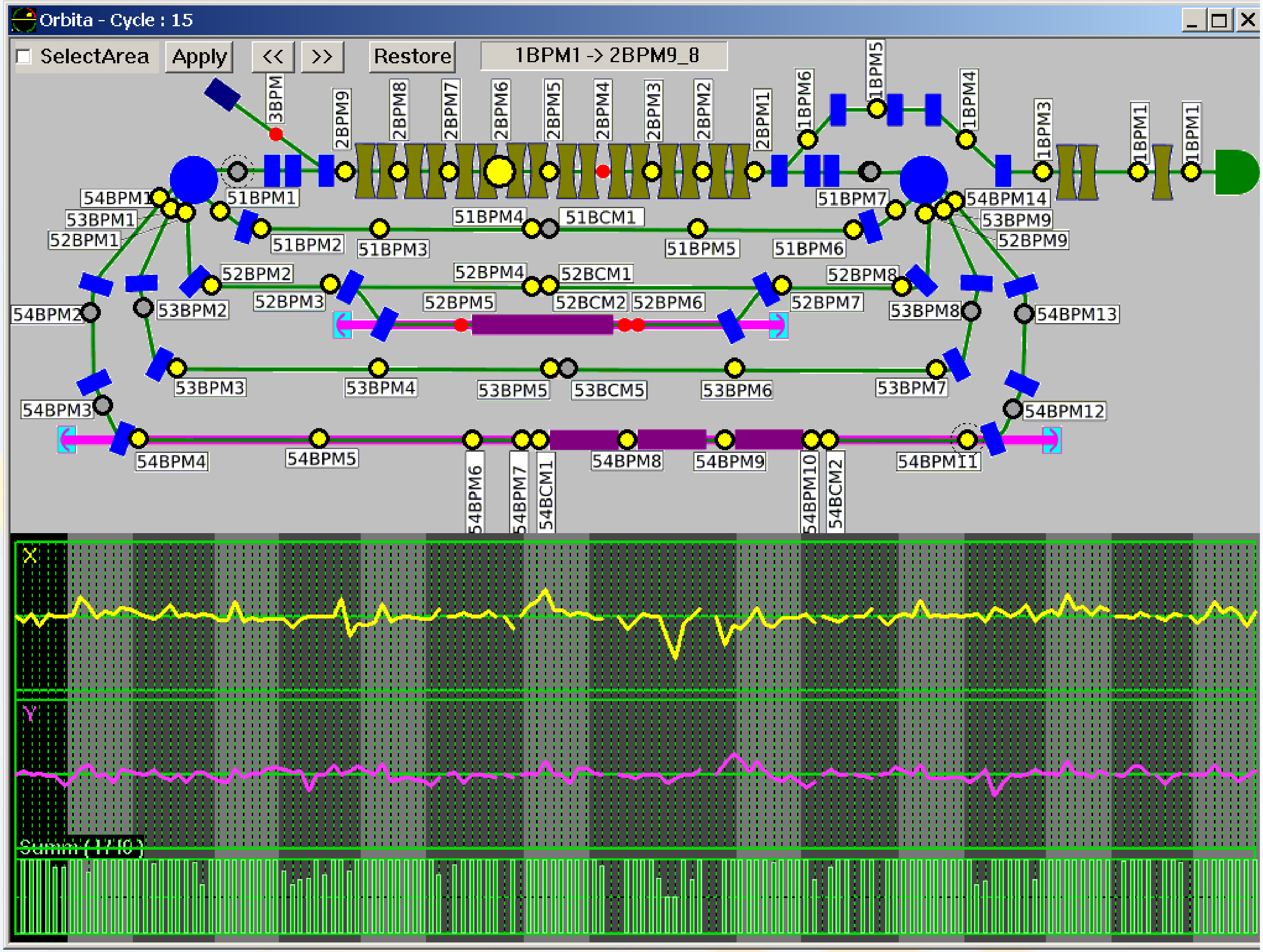

80% of the beam current goes to the dump

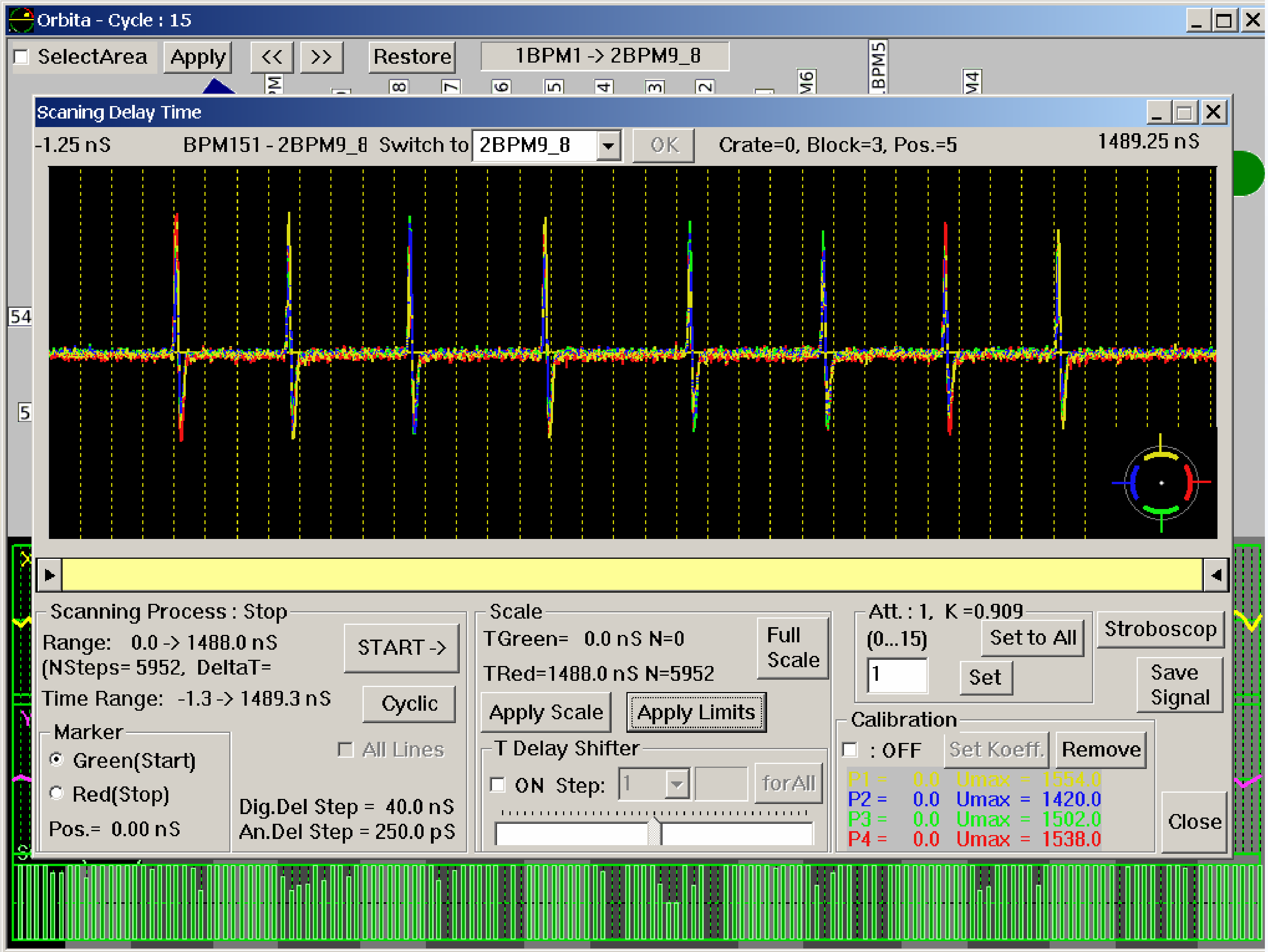

80% of the beam current goes to the dump

Current status

The first in the world multiturn ERL was commissioned and now it works for high power FEL (average power 0.5 kW in wavelength range 40-80 microns). The FEL radiation is delivered to exiting user stations.

Commissioning of the third stage ERL is in progress. The recuperation efficiency of 80 % is already achieved that allowed to increase the average current up to 1 mA.

Nearest plans

- Commissioning of the third stage ERL and FEL: lattice optimization; installation of the third FEL undulators; optical cavity design and production.
- Existing FELs stability and parameters improvement: modification of RF power generators; production of the new power supply for existing DC gun and new RF gun development.
- Working for users and new user stations development.

Thank you for your attention!